ResearchGate

See discussions, stats, and author profiles for this publication at: https://www.researchgate.net/publication/239943912

Biological detection by optical oxygen sensing

Article *in* Chemical Society Reviews · June 2013

DOI: 10.1039/c3cs60131e · Source: PubMed

CITATIONS
202

READS
1,179

2 authors:

Dmitri B Papkovsky
University College Cork
258 PUBLICATIONS **5,555** CITATIONS

SEE PROFILE

Ruslan Dmitriev
University College Cork
100 PUBLICATIONS **1,522** CITATIONS

SEE PROFILE

Some of the authors of this publication are also working on these related projects:

Project Development of a human cerebroid model of Alzheimer's disease View project

Project IGF-IR regulated genes in cancer View project

All content following this page was uploaded by Ruslan Dmitriev on 03 April 2015.

The user has requested enhancement of the downloaded file.

Chem Soc Rev

RSC Publishing

REVIEW ARTICLE

View Article Online
View Journal

Biological detection by optical oxygen sensing

Cite this: DOI: 10.1039/c3cs60131e

Dmitri B. Papkovsky* and Ruslan I. Dmitriev

Recent developments in the area of biological detection by optical sensing of molecular oxygen (O_2) are reviewed, with particular emphasis on the quenched-phosphorescence O_2 sensing technique. Following a brief introduction to the main principles, materials and formats of sensor technology, the main groups of applications targeted to biological detection using an O_2 transducer are described. These groups include: enzymatic assays; analysis of respiration of mammalian and microbial cells, small organisms and plants; food and microbial safety; monitoring of oxygenation in cell cultures, 3D models of live tissue, bioreactors and fluidic chips; *ex vivo* and *in vivo* O_2 measurements; trace O_2 analysis. For these systems, which enable a range of new bioanalytical tasks with different samples and models in a minimally invasive, contact-less manner, with high sensitivity, flexibility and imaging capabilities in 2D and 3D, relevant practical examples are presented and their merits and limitations discussed. An outlook of future scientific and technological developments in the field is also provided.

Received 8th April 2013

DOI: 10.1039/c3cs60131e

www.rsc.org/csr

Published on 18 June 2013. Downloaded by University College Cork on 18/06/2013 10:57:28.

1. Introduction

Molecular oxygen (O_2) is of paramount importance for living organisms and biological systems. For anaerobic organisms O_2 is generally toxic and must be excluded or controlled accurately at low levels.[1,2] Obligate anaerobes die in the presence of O_2 or create microoxic zones, whereas facultative anaerobes can use both anaerobic respiration (fermentation) and aerobic respiration for growth.[1] In photosynthetic organisms O_2 fluxes reflect their efficiency and metabolic state (light-dependent and dark processes).[3,4] Aerobic cells and organisms require a constant

Biochemistry Department, University College Cork, College Road, Cork, Ireland. E-mail: d.papkovsky@ucc.ie; Fax: +353-21-490-1698; Tel: +353-21-490-1698

Dmitri B. Papkovsky

Dmitri B. Papkovsky is a Professor of Biochemistry at the University College Cork, Ireland, where he has been working since 1997. He graduated from the Chemistry Department of Moscow State University (1982) and received his PhD from the Institute of Biochemistry (1986). Prof. Papkovsky has 120+ primary papers, over 20 reviews and book chapters. Several sensor systems and applications developed in his group have been commercialised. His current research interests include phosphorescent porphyrin dyes and materials; sensing and imaging of O_2; biological roles of O_2 and uses as a marker of cellular (dys)function; fluorescence spectroscopy, time-resolved fluorescence, bioimaging. His website is: http://publish.ucc.ie/researchprofiles/D003/dpapkovsky.

Ruslan I. Dmitriev

Ruslan I. Dmitriev, born in Yeniseysk, Russia in 1981, received his MSc degree in Chemistry and Technology from Lomonosov Moscow State Academy of Fine Chemical Technology in 2004. He completed his PhD in bioorganic chemistry in 2008 at Shemyakin-Ovchinnikov Institute of Bioorganic Chemistry, where he studied membrane ion-transporting proteins and protein interactions. His postdoctoral work at the Biochemistry Department, University College Cork, Ireland has been focused on development and biological applications of novel small molecule and nanoparticle based phosphorescent probes for cellular O_2. Current research interests include bioconjugate chemistry, new probe and assay development, mitochondrial dysfunction, metabolism and hypoxia research.

Published on 18 June 2013. Downloaded by University College Cork on 18/06/2013 10:57:28.

supply of O_2 to generate energy in the form of ATP, perform the necessary physiological functions and drive numerous enzymatic reactions which convert metabolic substrates and produce vital products.[5] O_2 levels in mammalian tissue are normally tightly regulated and maintained within narrow physiological limits.[6–8] Higher eukaryotic organisms including mammals and humans have developed special systems to store, transport and regulate O_2 in tissues by means of haemoglobins, myoglobins, red blood cells and vasculature. A decreased O_2 or imbalance between O_2 supply and demand may lead to pathological states and ultimately death of the cell and whole organism.[7] On the other hand, aerobic cells also possess oxygen-independent energy production pathways (*e.g.* glycolysis, Krebs cycle, glutaminolysis) which allow them to survive stress conditions by compensatory regulation and adaptation of their energy requirements and metabolism to changing environments. Living organisms are also able to 'sense' low and high O_2 (hypoxia and hyperoxia causing energy and oxidative stress, respectively) and respond in an adaptive manner and thus survive. However maladaptive responses to O_2 are also common, *e.g.* the Warburg effect in cancer cells, tissue remodelling. Recent research also demonstrates the pivotal role of O_2 regulation in plants,[9] microbes and the complex interspecies communities such as deep sea vents, soil or gut biota.[10]

O_2 can therefore be viewed as an informative marker of the presence, viability, metabolic status and physiological behaviour of living systems that consume, release or depend on O_2 levels in the environment. The generic nature of this marker can be used to probe many functional characteristics of biological specimens, their behaviour under various conditions (both internal and external), metabolic parameters and responses to stimuli, drug treatment or transformation. Direct and indirect involvement in the many functions of cells, tissues and whole organisms, make O_2 one of the most important analytes, particularly in general cell biology, tissue and animal physiology, detection of aerobic cells, biomedical and clinical diagnostics, microbial safety, food science, environmental monitoring, and many other areas of science and human practice.

As an analyte, O_2 is a small, non-polar, gaseous, paramagnetic molecule, which has moderate solubility in aqueous solutions. Under air-saturated conditions (20.86% O_2, normal atmospheric pressure) dissolved O_2 concentration is 219 μM at 35 °C, and is strongly influenced by temperature and salinity (*e.g.* 166 μM at 5% salinity, 35 °C).[1,11] Unlike other biological analytes such as ions, pH, metabolites, cellular markers, O_2 is not confined in a specific compartment of the cell or the biological sample, it diffuses fast across cell membranes, tissues, solution phase and even solid matter. Many polymers have moderate and high permeability and solubility for O_2, and this must be taken into account, especially for common plasticware made of polystyrene, polycarbonate and silicone.[11] Diffusion coefficient of O_2 in aqueous media at 25 °C is 2×10^{-5} cm^2 s^{-1}, and O_2 capacity of air is approximately 50 times higher than for water.[12] As a consequence, altered mass exchange or contact with the gaseous phase (ambient air) may have a profound impact on O_2 measurements and skew the results. It is also impossible to 'freeze' homeostatic O_2 levels within the sample and analyse them afterward (*post factum*). Therefore, the sensor, the detection system and the biological sample need to be carefully tuned to each other, so that they operate in an analytically plausible manner and under biologically relevant conditions.

Realisation of the variety of analytical tasks with biological samples of different types and characteristics requires a spectrum of dedicated sensor materials, analytical methodologies, measurement instrumentation and accessory tools. A large number of different platforms have been developed for O_2 detection and quantification in biological specimens, among which optical and particularly quenched-luminescence sensing techniques represent an important and very versatile group.[13–15]

The scope of this review is rather broad as it spans across various roles of O_2 in biological systems, analytical applications of this biomarker, new biological knowledge revealed by its use, and advancement of the optical O_2 sensing technology and materials. It is difficult to cover all the aspects in equal detail, so we had to focus on the most important developments directly related to biological detection, and perhaps leave aside some excellent work on sensor materials, analytical methodologies and detection platforms, if at this stage they do not demonstrate novel biological data or clear practical advances in biological detection. The number of studies in the area, the groups producing these results and chemical, life science and medical journals publishing them are growing exponentially.

In this review, we mainly analyse the new *applications* of quenched phosphorescence O_2 sensing in the area of biological detection developed over the last 5–7 years, examining their main findings, merits, limitations and *status quo*, and trying to identify the directions of future research. The details of sensor materials and detection systems used in these applications will be discussed only briefly, these aspects are well covered in recent reviews.[13,16–21] The authors would also like to apologise for possible oversight or exclusion from this collection of some studies that other researchers may consider relevant to the subject.

2. O_2 detection techniques

Traditional O_2 quantification relies on sampling and analysis by chemical (Winkler titration[22]), physical (cartesian diver,[23] manometric[24]) or instrumental (gas chromatography[25]) methods. However, high demand for continuous monitoring, minimally or non-invasive measurements, *in situ* and *in vivo* analyses and imaging of O_2 in complex biological samples have led to the development of a spectrum of new detection platforms. These include the relatively simple and low cost electrochemical sensors (Clark-type O_2 electrode[26]) actively used nowadays, optochemical sensors and biosensors, which have already become indispensable in many laboratory and industrial applications,[13] and more sophisticated instrumental techniques such as Electron Paramagnetic Resonance,[27] functional Magnetic Resonance Imaging,[28] Positron Emission Tomography,[29] pulse oximetry,[30] and intrinsic optical signal imaging.[31] In this family, optical techniques and particularly phosphorescence,[32,33] fluorescence,[34]

 This journal is © The Royal Society of Chemistry 2013

Published on 18 June 2013. Downloaded by University College Cork on 18/06/2013 10:57:28.

Table 1 Common optical techniques used for O_2 detection in biological samples

Method[ref.]	Detection principle	Probe type	Advantages	Limitations
Luciferase reporter system[35]	O_2-dependent expression and bioluminescence of luciferase enzyme	Endogenous luciferase and substrate	Sensitive, easy to measure	Not quantitative, requires cell transformation (reporter gene) and substrate
Phosphorescence quenching[33]	Quenching of phosphorescence of exogenous probe introduced in the sample	Synthetic phosphorescent materials	Direct, accurate, quantitative method. Stable calibration. Various read-out parameters (intensity, lifetime, ratiometric intensity). Many different formats and applications including imaging	Exogenous substance in the sample. Possible toxicity, altered function, O_2 photoconsumption
Colorimetric indicators[326–328]	Changes in absorption upon O_2 binding or red-ox reactions	Exogenous dyes	Possibility of visual detection, simple chemistry	Slow response, interferences, low resolution, instability. Not fully reversible
Hypoxia stains misonidazole and pimonidazole[38,39]	Administration of a redox dye, visualisation of hypoxic areas (dye accumulation) by immunohistochemistry	Bioreducing dye	Staining of hypoxic regions tissue. Analysis of tissue samples *post mortem*	Indirect, end-point method. Does not allow for quantification or real-time monitoring of O_2
Hypoxia staining with fluorescent protein expressed under HIF promoter[329]	Fluorescent protein is expressed in cells upon activation of HIF signalling	Red fluorescent protein or its modifications	Direct and real-time staining of hypoxic regions. No need in antibodies	Viral transfection is preferable. Dependence on activity of HIF system within the cell (cell-specific). Semi-quantitative
Hypoxia staining with fluorescent probes[254,330–332]	Administration of redox dye, visualisation by fluorescence	Redox dye, convertible by nitroreductase or related endogenous enzymes	Direct and real-time staining of hypoxic regions. No need in antibodies	Semi-quantitative. Dependence on the endogenous enzyme activity
Measurement *via* fluorescence of GFP constructs[34,40,333]	Detection of reversible (''photoactivated'') red-shifted O_2 dependent fluorescence	Green fluorescent protein or its modifications	Intracellular, *in vivo* imaging. Targeted delivery to cellular compartments	Require genetic manipulation or cell transfection. Low sensitivity to O_2 (detectable at $<2\%$ O_2), semi-quantitative. Dependence of probe maturation on O_2
Delayed fluorescence of PPIX[37]	Dynamic quenching of PPIX delayed fluorescence by O_2	Overproduced endogenous PPIX upon administration of 5-aminolevulinic acid	Minimally invasive. Direct measurement of mitochondrial O_2. No toxic effects reported	Weak signals, low S/N requires cell stimulation. Low photostability of PPIX. Applicable only to eukaryotic cells and tissues
Photoacoustic spectroscopy[36]	Transient absorption of excited triplet states of an O_2 sensitive dye	Exogenous dyes with long-lived triplet states (*e.g.* metalloporphyrin or methylene blue)	Deep tissue penetration. 3D imaging	Two NIR lasers (exciting and probing). Complex and expensive set up. Substantial doses of the probe

bioluminescence,[35] and photoacoustics[36] based O_2 detection represent a large and important group.

The intrinsic properties of the O_2 molecule make its direct detection rather difficult. Therefore, special 'indicator substances' are employed for selective and sensitive detection of O_2 in complex samples, which produce a characteristic and easily detectable signal without the need for tedious sampling and processing steps. Such indicators can be *endogenous* chemical or biological molecules present in the sample, for example haemoglobin in red blood cells[30] or protoporphyrin IX (PPIX[37]). Genetically encoded fluorescent protein constructs[34] can be introduced into cells by DNA or viral transfection or cell transformation. Otherwise, exogenous, synthetic indicators, represented by O_2-sensitive dyes, conjugates, supramolecular structures and composite materials (coatings, particles, probes) on their basis, can be introduced in the test sample to achieve O_2 detection.[18] The indicator produces a characteristic response as a result of a physico-chemical (binding, reduction–oxidation), biological (accumulation of glucose analogues or bioreduction of redox dye in hypoxic cells[38]) or photophysical (phosphorescence quenching,[33] acoustic,[36] delayed fluorescence[37]) process that is linked to O_2 concentration or to the related parameter of the sample. Table 1 gives an overview of different optical methods used for O_2 detection, highlighting their attractive features and limitations.

Unfortunately, many of these systems for O_2 detection appear to be indirect and/or mediated by the complex (bio)-chemical reactions or processes which are slow, not fully reversible, non-stoichiometric or influenced by many factors (Table 1). Some of these methods are tailored to specific applications with predefined analytical specifications (medical or diagnostic), which require special samples, measurement conditions and instrumentation, or provide a semi-quantitative or end-point O_2 readout.[29,30,38,39] Endogenous O_2 indicators are also in small numbers[37,40] and have limited use. In this regard, O_2 sensors and probes based on quenching of exogenous photoluminescent dyes possess many attractive features and advantages over the other platforms for O_2 detection.[18]

3. O_2 sensing by phosphorescence quenching

Since its discovery,[41] quenched-phosphorescence O_2 sensing has evolved as a powerful analytical method with long-ranging applications. First O_2 sensing systems introduced in 1960s[32] and 1980s[33] targeted the very demanding biomedical applications.

Published on 18 June 2013. Downloaded by University College Cork on 18/06/2013 10:57:28.

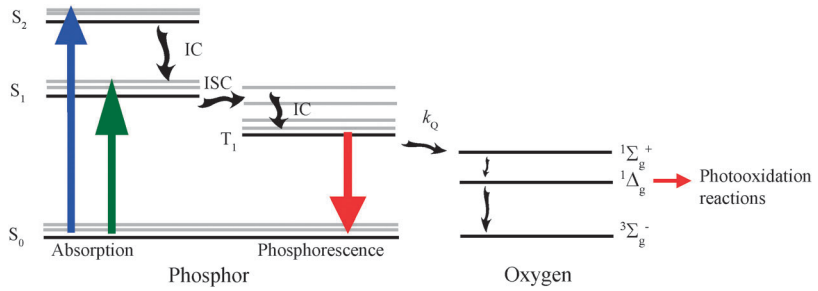

Fig. 1 Simplified Jablonski diagram showing the main energy transitions during the process of phosphorescence quenching by O_2. S_0, S_1, S_2 – ground state, first and second excited singlet states of the indicator, and T_1 – its excited triplet state. IC – internal conversion; ISC – intersystem crossing.

One was monitoring of blood oxygenation during intensive care by fibre-optic microsensors with solid-state O_2-sensitive coatings and fluorescence intensity measurements.[42,43] Another was the phosphorescent lifetime based analysis of tissue oxygenation using a soluble probe, tailored for the *in vivo* O_2 imaging format.[33,44]

Although providing a step change in O_2 determination, the uptake of these technologies was rather slow. Partly because first sensing materials and detection approaches were far from being optimal, measurement instrumentation was not readily available, and applications themselves required special technical expertise and detailed validation to demonstrate their practical benefits. During the 1990s and 2000s, optical O_2 sensor technology underwent major development, which revolved around its main building blocks: sensor materials and indicator dyes, detection instrumentation and measurement schemes, and analytical methodologies. Quenched-phosphorescence O_2 sensing has largely benefited (and continues to do so) from the technological advancements in allied disciplines, particularly synthetic, polymer and supramolecular chemistry,[16,17,20,21] semiconductor optoelectronics, fluorescence spectroscopy,[45] chemical biology[46] and nanotechnology,[47,48] optical and bio-imaging.[49–51] This cross-fertilisation produced a range of advanced sensor chemistries, materials, measurement approaches and detection platforms.[16] Intensive R&D has addressed the main bottlenecks of the O_2 sensor technology and produced new tools and systems with enhanced capabilities, some of which have become commercial products.[13,18,20,52–54] Development of new applications and their dissemination are now keys for harvesting the full potential of optical O_2 sensing.

3.1. Detection principles

Quenched-phosphorescence O_2 detection relies on direct, non-chemical, reversible sensing of O_2 *via* a *photochemical* process of collisional quenching of excited state indicator dye molecules by molecular oxygen (Fig. 1). Upon light excitation, the luminophore absorbs photons and, through the processes of internal conversion and intersystem crossing, quickly relaxes to the excited triplet state. The emission from the triplet state is generally slow (a forbidden process which requires a change of spin). As a result, some excited dye molecules undergo quenching through collisional interaction with O_2 which reduces the yield and lifetime of the phosphorescence in a concentration-dependent manner. It is considered that the paramagnetic ground state O_2 molecule ($^3\Sigma g^-$, open-shell triplet state) accepts energy from the luminophore's excited triplet state, recovering the ground state luminophore and generating a very short lived state ($^3\Sigma g^+$) and subsequently singlet oxygen ($^1\Delta g$).[16] Singlet oxygen, the main product of the quenching process, has relatively short lifespan in condensed media and high reactivity. It quickly deactivates back to the ground state O_2 (through interaction with solvent molecules, but also showing weak phosphorescence at 1270 nm[55]), or reacts with neighbouring chemical structures causing their oxidation.[56]

Photoluminescent O_2-sensitive materials are usually based on synthetic indicator dyes (macrocyclic complexes of heavy metal ions) with long-decay emissions (phosphorescence or delayed fluorescence) and lifetimes in the microsecond range. In recent years, many good reviews were published,[16–19,21,57] which describe over a hundred of different indicator structures and their photophysical and O_2 sensing characteristics. Considering that such indicators can be used in different types of sensor materials, this gives us a pool of hundreds of different O_2-sensors. However, when it comes to specific applications, many of these indicator dyes and sensor materials become redundant or obsolete. In fact, the field of O_2 sensing is currently dominated by a rather small group of dyes, which have spectral and O_2 sensing characteristics, availability, costs, analytical performance, biocompatibility and the level of practical validation far superior to the other members. Most popular phosphorescent dyes are shown in Table 2 and Fig. 2.

For many research and laboratory applications, O_2 indicators emitting in the visible range (550–700 nm) are very appropriate, especially for screening of biological samples of similar type such as cell cultures. Thus, $Ru(dpp)_3^{2+}$, $Ir(C_s)_2(acac)$, PtCP and PtPFPP dyes are compatible with standard fluorescence spectrometers and readers and can be measured even in simple intensity mode to trace relative changes in concentration or O_2 consumption rate. Some of these dyes also allow lifetime-based O_2 detection on such instruments, which makes them more efficient, robust and quantitative and therefore preferred. For the dyes used on a disposable basis on such instruments, photostability is not so critical, however high brightness ($\varepsilon\Phi$ product, Table 2) is always an advantage. Spectral sensitivity of photodetectors should be considered as it usually declines sharply at long wavelengths.

This journal is © The Royal Society of Chemistry 2013

Table 2 Popular O_2-sensitive photoluminescent dyes and their characteristics (taken from ref. 16, 61 and 334)

Indicator dye	λ_{max}^{exc} (nm)	λ_{max}^{em} (nm)	τ_0 (μs)	Brightness, ($\varepsilon\Phi$) (M^{-1} cm^{-1})	Photostability
PdTCPP	415, 524	690	640	1900	Moderate
PdTCPTBP	442, 632	790	251	6000	Moderate
PtPFPP	390, 504, 538	647, 710	60	28 424	High
PtTPTBPF	430, 615	773	50	87 600	High
$[Ru(dpp)_3]^{2+}Cl_2$	463	618	6.4	10 467	High
PtCP	380, 535	650	67	56 000	Modest
$Ir(C_s)_2(acac)$	472, 444	563	11.3	50 112	Modest

Abbreviations: PdTCPP – Pd-*meso*-tetra-(4-carboxyphenyl)-porphyrin dendrimer; PdTCPTBP – Pd-*meso*-tetra-(4-carboxyphenyl)tetrabenzoporphyrin dendrimer; PtPFPP – Pt(II)-tetrakis(pentafluorophenyl)porphine; PtTPTBPF – Pt-*meso*-tetra-(4-fluorophenyl)tetrabenzoporphyrin; PtCP – Pt-coproporphyrin; $Ru(dpp)_3$ – tris(4,7-diphenyl-1,10-phenanthroline)ruthenium(II) chloride; ε – molar absorptivity, Φ – phosphorescence quantum yield. τ_0 – unquenched phosphorescence lifetime.

Published on 18 June 2013. Downloaded by University College Cork on 18/06/2013 10:57:28.

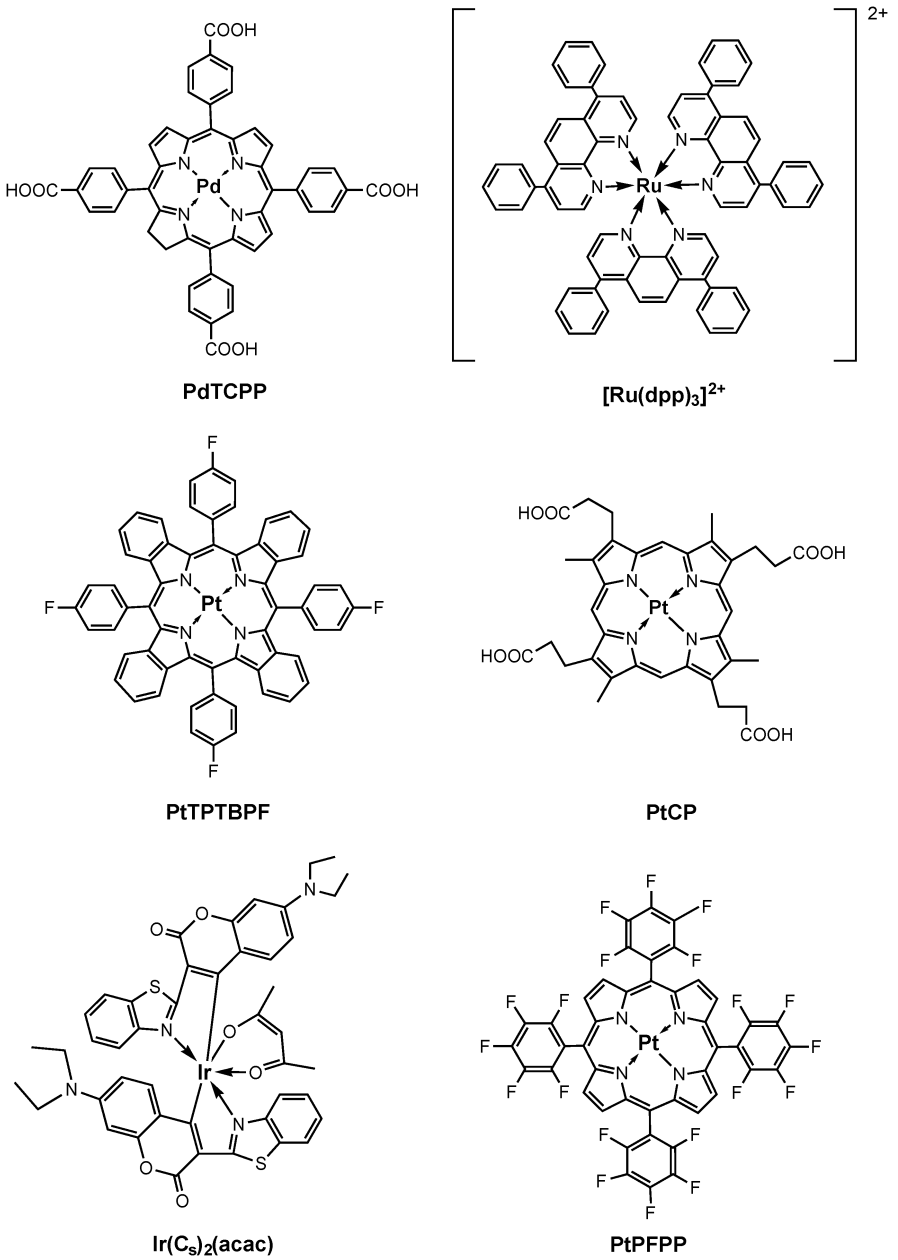

Fig. 2 Chemical structures of some O_2-sensitive indicator dyes, described in Table 2.

Published on 18 June 2013. Downloaded by University College Cork on 18/06/2013 10:57:28.

For measurements in animal tissue and complex specimens (coloured, highly scattering and fluorescent samples), the choice is driven towards the indicators that are excitable and emitting in the red and very-near infrared spectral region (600–900 nm), such as benzoporphyrins. In high-resolution microscopy imaging, high photostability and brightness are the main criteria for indicator selection, which point towards PtPFPP and PtTPTBPF dyes[16] or systems with light-harvesting antennae.[58–60] Shorter emission lifetimes are also preferred for imaging, providing faster acquisition times and better temporal resolution in time-lapse experiments. In this regard, Pt-porphyrins are better than Pd-complexes which have 3–10 times longer τ_0 (and K_{s-v}) values.[16] Ru-dyes are also attractive, but they often show low sensitivity to O_2, cyto- and phototoxicity[57] due to their cationic and non-biogenic nature, making them less preferred than porphyrins.

The alternative O_2-sensitive dyes have less favourable photophysical properties (highlighted in Table 2) or biocompatibility, making them hard to compete. Nonetheless, the relatively small group of high-performance indicators provides the basis for a broad range of O_2-sensitive materials, the main groups of which are outlined in Table 3. Notably, Tables 2 and 3 are non-exhaustive, meaning that new 'blockbuster' indicators and sensor materials may appear in the future.

Photophysical and O_2 sensing properties of an indicator dye are dependent on its micro-environment (*e.g.* polymer matrix medium or sensor material), macro-environment and properties of the sample (temperature, presence of other quenchers, light-absorbing components, and sometimes pH, ionic strength, binding agents[61,62]). This knowledge can be used to perform rational modification of the indicator, encapsulation/quenching medium or the method of incorporation in a sample and tune the properties of an O_2-sensitive material.[16,63] For example, sensitivity to O_2 and the measurement range are determined by the Stern–Volmer quenching constant which, in turn, is determined by the unquenched phosphorescence lifetime of the indicator and characteristics of encapsulation media. For example, Pt(II)-porphyrins (PtPFPP and PtCP) are more sensitive to O_2 than corresponding Pd(II) complexes.[18] The addition of a dendrimeric shell to the phosphorescent PdTCPTBP moiety linearized and stabilised its O_2 calibration, increased hydrophilicity and solubility in water, decreased τ_0 and quenching constant and protected from quenching interferences.[61,64]

Polymers are widely used as encapsulation and quenching media. Examples include common plastics (polystyrene, fluorinated polymers, polysulfone, polycarbonate, plasticized PVC), co-polymers, silicones, ormosils, sol–gels, and hydrogels. Proper selection of the polymer enables to achieve the desired specifications of sensor material, particularly its sensitivity, measurement range, response time, method of dye inclusion, biocompatibility, and sensor format (solid-state film coatings or nanoparticle probes). Polymer matrices with high permeability and diffusion of O_2 provide higher sensitivity.[21,47,63]

Furthermore, available indicator dyes and sensor materials can be bundled with other indicators, reporters or reference dyes to produce O_2 sensitive materials with new functional features. Examples include new supramolecular structures, bioconjugates, polymeric composites, nanoparticle formulations, and materials for multi-parametric analyses. These are covered in more detail in recent reviews.[32,33,45,48,49]

3.2. Practical realisation and measurement set-ups for optical O_2 sensing

With respect to analysis of biological specimens, the main measurement tasks include: (1) sample oxygenation, *i.e.* O_2 concentration; (2) O_2 consumption rate (OCR), *i.e.* O_2 flux associated with a biochemical process in the system; (3) spatial distribution and gradients of O_2 within the sample; and (4) dynamics of O_2 changes in time and space.

The need to perform various analytical tasks with different biological specimens by O_2 sensing has also led to the development of a number of measurement set-ups and detection options, which enable O_2 measurement in a sample to be carried out in a number of different ways. Some typical examples are presented in Table 4 and Fig. 3.

Fibre-optic (micro)sensors provide flexibility and miniaturization, allowing us to access small compartments of the sample and even penetrate into tissue (needle sensors). However the sensor is usually non-detachable,[20] which makes them invasive (minimally though).

Point measurement of O_2 can be realised by applying a solid-state sensor coating to a small area in an assay vessel in contact with a liquid sample or headspace.[20] In solid-state materials indicator molecules are shielded from quenching interferences with a gas-diffusion barrier (polymeric matrix), they do not contaminate the sample, have high specific signals that can be used in various environments and facilitate quantitative O_2 measurements even in intensity mode. These spot sensors are relatively easy to fabricate and tune, and they can be measured from outside the vessel, *i.e.* contactless. However, they are not very suitable for studying complex respiring samples with profound heterogeneity and localised O_2 gradients.

Soluble probes can be distributed across respiring objects, such as cultured cells or tissue to enable O_2 analysis in different parts of the sample. They can be used without much adaptation in various assay substrates, miniature samples, and even be introduced into the cell or the 3D respiring sample such as tissue or whole animal. Such probes provide the highest degree of flexibility. However, their signals are usually much lower than for solid-state sensors (the latter can accommodate up to 1% w/w of the dye[16]), they contaminate the sample, and are harder to use on a large scale and with macroscopic samples.

While solid-state O_2 sensors and probes have their merits and limitations, micro- and nano-particle sensors combining the features of both can overcome the limitations. In addition, magnetic O_2-sensitive microparticles can be distributed in the sample, but then concentrated and manipulated with a magnet.[65]

In some of the set-ups, solid-state (micro)sensors and probes are interchangeable and provide similar analytical performance (*e.g.* OCR assays in cuvettes or microplates with localised sensor coating or probe distributed evenly). Measurement of relatively uniform biological samples (microbial, mammalian cells) is

 This journal is © The Royal Society of Chemistry 2013

Published on 18 June 2013. Downloaded by University College Cork on 18/06/2013 10:57:28.

Table 3 The main types of phosphorescent O_2 sensitive materials

O_2-sensitive material	Measurement tasks	Advantages	Limitations
Thin-film solid-state sensors:			
Non-detachable solid-state (micro)sensors	Point measurement of dissolved and gaseous O_2 concentration	Minimally invasive. Scanning capability (with micromanipulator). No sample contamination, multi-point systems (2–4 channels)	Less durable and robust than spot sensors. Fragile, invasive, costly
Detachable spot sensors (coatings, inserts)	Point measurements of dissolved or gaseous O_2 concentration	Provide non-invasive, contact-less sensing, disposable and long-term use. No sample contamination, high optical signals, low cost, robustness. Many sensors can be probed with one instrument	Integration in sample is not easy. Limited flexibility and applicability – adhesion, solvents, microscopic samples. Point readings not always representative
Substrates with built-in sensors (coated plates, tubes, flasks)	Process control, screening of multiple samples	Convenient, ready for use. Optimised for disposable use in certain applications. Affordable	Limited flexibility, suit only certain applications. Assay redesign is difficult
Planar optodes (sensor sheets)	2D visualisation of O_2 distribution and gradients	2D imaging capability	Fragile sensor films, require solid support. Difficult interfacing with samples
Soluble probes:			
General use (macro)molecular probes	Measurement of dissolved O_2 in bulk samples	Compatible with various samples, substrates and tasks, especially small samples and screening applications. Adjustable signals and formats	Contaminate samples. Weaker signals than with solid-state sensors
Micro- and nano- particle probes	Measurement of dissolved O_2 in bulk samples	Easy use by dispensing. Allow manipulation (*e.g.* magnetic beads). Flexible, easy to manufacture. Increased brightness and photostability	Contaminate samples. Stability, reproducibility and aggregation issues
Targeted probes (cell/tissue-permeable)	Cell/tissue penetration or binding. Control of local oxygenation and O_2 gradients	Allow analysis of cell populations, tissue and individual cells	May impair cellular function. Cell-specific accumulation and distribution
Imaging probes	Measurement of vascular and tissue O_2	High photostability, low intrinsic and phototoxicity, sufficient brightness and retention in cells	Often show cell specificity, lack of photostability, limited validation
Multi-functional and multi-modal probes	Provide additional reference signal or parameter	Increased flexibility, more stable (ratiometric) and multi-parametric measurements	Complex synthesis, high costs. Stability, batch-to-batch variability
In vivo probes	Allow use in live animals and tissues	Improved safety and biocompatibility, low toxicity, high level of validation	Require complex measurement set up and animal licences. Many accessory techniques

Table 4 Main measurement set-ups used in optical O_2 sensing with biological specimens

Measurement set-up	Brief description and sensor type	Main applications
Fibre-optic probe – microsensor	Optical fibre with sensor material on the tip, and protective cladding (optional). Normally solid-state coating, or probe solution in a microchamber on the tip	Point monitoring of sample O_2. OCR measurement. Scanning of O_2 distribution (with micromanipulator)
Air-tight cuvette	Sealed cuvette (no headspace, air-tight), with or without stirrer. Extracellular probe or solid-state sensor (sticker or microsensor)	OCR measurements with enzymes, isolated mitochondria, suspension cells, small organisms
Partially sealed cuvette or chamber	Microplate wells sealed with mineral oil. Capillary cuvettes,[93] vials with sensors,[92] extracellular probes or solid-state sensor coatings	Respiration and OCR measurements with cells, enzymes, small organisms isolated mitochondria. Analysis of cell metabolism, bioenergetics, drug treatment, cell physiology
Biochips with static samples	Sealable microplate,[92] XF analyser system,[105] microchannel biochips[292]	Respiration and OCR measurements with cells, enzymes, small organisms isolated mitochondria. Analysis of cell metabolism, bioenergetics, drug treatment, cell physiology
Fluidic systems and perfusion cells	O_2 measurement under flow conditions in a chamber with biological material. Extracellular and intracellular probes, solid-state sensor coatings and microsensors[173]	O_2 consumption measurements. Responses of cell and tissue samples to stimulation, drug treatment, hypoxia, *etc.*
Open samples in contact with atmosphere	An open plate or imaging mini-dish with respiring samples, in medium exposed to gaseous atmosphere. Mostly intracellular probes[18]	*In situ* control of oxygenation in cells, spheroids, tissues. Monitoring of steady-state oxygenation of cells and respiratory responses to metabolic stimulation. Studies of cell physiology and hypoxia. O_2 imaging
In vivo O_2 measurements	O_2 sensor/probe and detection system are tailored to a particular biological model and measurement task[18,75]	Levels, maps of O_2 concentration, their dynamics. Physiological studies

Published on 18 June 2013. Downloaded by University College Cork on 18/06/2013 10:57:28.

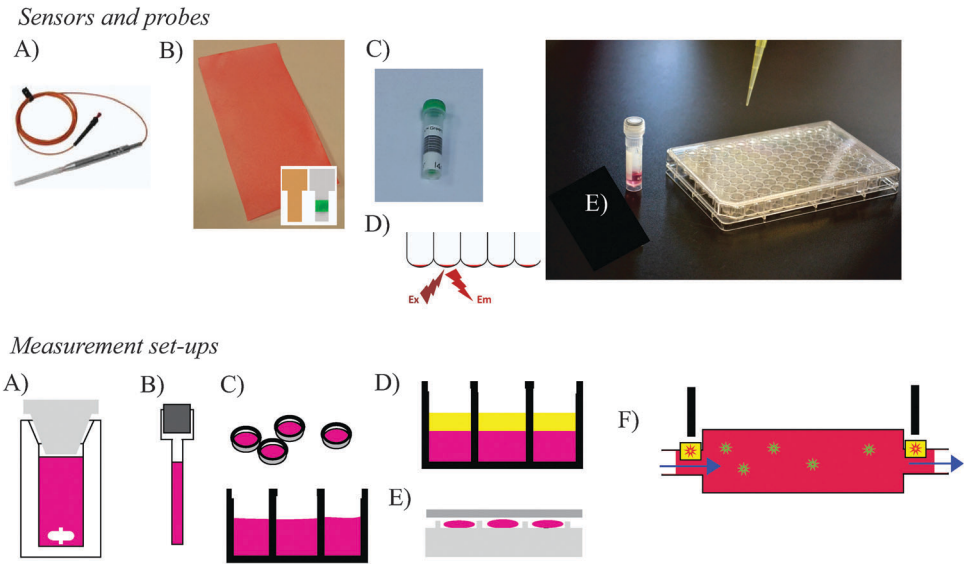

Fig. 3 Examples of common materials and measurement set-ups used for O_2 sensing in biological samples. Sensors and probes: (A) fibre-optic micro-sensor. (B) Planar sensor sheet and stickers with sensor dots. (C and D) Vial and microplate with sensor coating and measurement set-up. (E) Soluble probe used with standard microplates. Measurement set-ups: (A) sealed stirred cuvette. (B) Glass capillary with liquid barrier; (C) open microplate and imaging mini-dishes. (D) Microplate wells sealed with oil. (E) Low-volume sealable microplate. (F) Perfusion chamber, can operate under flow or static conditions with soluble (green) or solid-state sensors (yellow-red).

well developed and some applications are becoming standard, such as cell-based assays, drug screening, microbial tests and bioreactor monitoring. In other cases with complex and non-standard samples, such as whole organism ecosystems, micro-sensors, customisation of both the O_2 sensor/probe and detector parts is often required, which may be minor or very significant.

For quantitative monitoring of O_2 concentration using a sensor, it is necessary to establish the relationship between the measured optical parameter and O_2 concentration, *i.e.* calibration. The main read-out parameters in optical O_2 sensing are phosphorescence intensity (I) and lifetime (τ). They relate to O_2 concentration according to the Stern–Volmer equation:[66]

$$I_0/I = 1 + K_{S\text{–}V}[O_2] \quad \text{or} \quad \tau_0/\tau = 1 + K_{S\text{–}V}[O_2] \qquad (1)$$

$$[O_2] = (I_0/I - 1)/K_{S\text{–}V} \quad \text{or} \quad [O_2] = (\tau_0/\tau - 1)/(k_q\tau_0). \qquad (2)$$

The intensity and lifetime values at zero O_2 are designated I_0 and τ_0, while the sensitivity of O_2-sensitive material is determined by the quenching constant ($K_{S\text{–}V}$), which is a function of τ_0, the immediate environment of the dye, sterical factors and temperature (expressed *via* the bimolecular quenching rate constant, k_q).[66] For heterogeneous sensor materials and systems with non-ideal behaviour, more complex mathematical equations or fitting functions are used.[67] For the dual-fluorophore sensor systems, the intensity ratio of the O_2-insensitive and O_2-sensitive signals (I_1/I_2) is used for quantitation, this relationship resembles linearised Stern–Volmer.[21,68,69] Typical O_2 calibrations are shown in Fig. 4. Depending on the sensor material, instrumentation and the biological sample, calibration procedures may vary. Specific examples can be found in ref. 62, 70 and 71.

A broad variety of O_2 sensitive materials having different physical states, spectral characteristics, sensitivity to O_2, chemical–physical properties, and biocompatibility, is further augmented by the versatile photoluminescent detection. This allows design of simple, portable and affordable (bio)analytical systems for in-field, *in situ*, or laboratory use which can be operated by non-skilled personnel,[20,72] as well as sophisticated equipment tailored to a particular measurement task or application.[73,74] O_2 sensors can also be integrated in existing widely available detection platforms and multi-functional instrumentation,

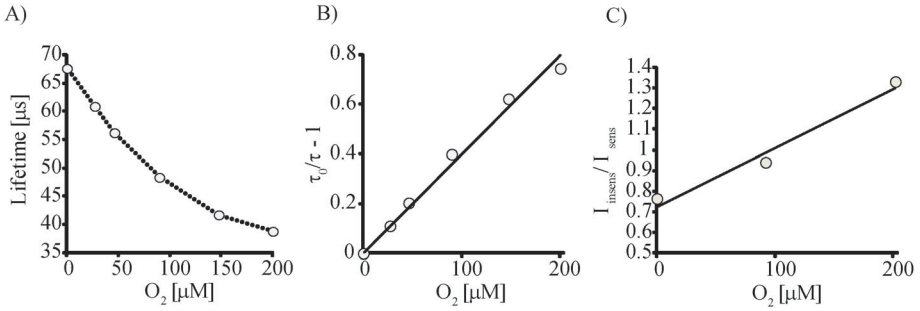

Fig. 4 Examples of calibrations of O_2 sensing materials operating in lifetime (A and B) and ratiometric intensity modes.

 This journal is © The Royal Society of Chemistry 2013

Published on 18 June 2013. Downloaded by University College Cork on 18/06/2013 10:57:28.

particularly conventional fluorescence readers and spectrometers, live cell and *in vivo* imaging systems. Similar to fluorescent bioimaging, multi-photon excitation is a preferred mode for O_2 sensing and imaging deep into tissue.[75]

Sensor intensity signals can be influenced by many parameters including dye concentration, measurement geometry, optical properties of the sample, drift of optoelectronic components, and photobleaching. Therefore, stable and precise calibration is difficult to achieve. These instability issues can be addressed using the sensors containing an additional spectrally distinct dye (O_2-insensitive reference) and ratiometric measurements at two different wavelengths. This compensates for many of the above factors,[68] though not completely.[21,76,77] Phosphorescence lifetime-based sensing is rather insensitive to variations of indicator concentration and experimental conditions that can influence intensity signals, it generally provides more stable measurements and enables to use once-off calibration.

Phosphorescence lifetime-based sensing schemes require more specialised instrumentation, with time-gated or frequency-modulated excitation and time or phase correlated detection, respectively.[78] Such platforms are also quite common in biomedical research. They enable assessment of biological activity and functional characteristics of different biological samples in a highly informative and versatile manner. Still, instrumental errors, environmental factors and measurement artefacts can lead to differences in experimental results and calibrations, so it is highly recommended to perform critical assessment, testing and calibration for such systems.

General instrumentation and data processing for phosphorescence intensity and lifetime-based O_2 sensing are described in many reviews,[20,45,51,79,80] and will not be discussed in detail here. At the same time, new detection systems and set-ups for specific biological application appearing with high frequency will be discussed in Section 4. The large leap in digital imaging equipment over the last few years, from high-spec gated CCD cameras to low-cost CMOS chips and mobile phone cameras, is also affecting the O_2 sensing area, with a number of systems and applications already described and commercialised.[81,82]

Last but not least, for many applications an important requirement for the O_2 sensor is that it does not bring or increase the risk of contamination for the sample under investigation. Sensors/probes usually need to be provided in a sterile form, while reusable sensors should withstand factory, on-line or at-line sterilisation. Standard sterilisation procedures, such as gamma irradiation, chemical sterilisation, heating or autoclaving, often cause damage to the sensor material,[83] so it has to be specially designed and optimised for this. Storage stability, biofouling,[84] transportation are other practical limitations for many O_2 sensors, especially liquid probes, and nanoparticle formulations.

4. Detection of biological activity by quenched-phosphorescence O_2 sensing

Biological applications of optical O_2 sensors often differ from their conventional industrial applications, in which measured O_2 concentration is the main parameter of interest. In biological detection, a primary signal from the sensor on its own rarely provides the sought information about the sample. To extract specific and physiologically relevant information, the input of additional sample parameters and criteria is usually required for the assay.

The additional information fed back into the sensor-based system can be, for example: key physical–chemical and biological characteristics of the sample and its micro- and macro-environment (*e.g.* mass, geometrical dimensions, temperature, humidity); known theoretical relationships between measured optical signals and sample parameters; initial or final conditions, results of experiments produced with control samples or artificial signal modulation; algorithms for converting sensor primary signal into biological parameters which account for key variables and potential sources of error.

This reflects the general strategy of analysing complex biological specimens by O_2 sensing, while it is the task of the operator to keep it to a reasonable minimum that ensures stable and robust measurements and generation of unambiguous end-results. Detailed optimisation of the measurement system and independent verification of results it produces are very important. Indeed, not paying due attention to these factors, many of which have biological nature, may lead to measurement artefacts, misinterpretation of experimental results or too broad generalisations (discussed in more detail in Section 4.13). If assay results are valid only for a particular condition or a sample type, this should be clearly specified. In other cases, primary optical signals can be applied for assessment, without calculating O_2 or OCR values.

In the following sub-sections we review the main groups of applications of quenched-phosphorescence O_2 sensing targeted at biological detection, assessment of activity and functional characteristics of biological specimens, with particular examples and their analysis.

4.1. Enzymatic assays

Living systems constantly maintain and reproduce themselves through a complex network of metabolic, biosynthetic and biodegradation pathways driven by enzyme-catalysed reactions, many of which are O_2 dependent. Even the reactions that do not directly consume or release O_2 are often coupled with other enzymatic reactions that are influenced by O_2. Quenched-phosphorescence O_2 sensors allow for investigation of enzymes that directly consume O_2. Indirect assessment, when the target enzyme-catalysed reaction is coupled with an oxidase consuming the product of the first reaction, is also possible.[13] Altogether, this provides a large scope for designing various enzymatic assays based on the monitoring of consumption or release of dissolved O_2. Such assays can be configured to perform: (1) analysis of enzyme substrates – key metabolites such as glucose, lactate, amino acids, cholesterol; (2) measurement of activity of clinically and industrially relevant enzymes; (3) mechanistic studies of enzymes, their substrates and inhibitors; and (4) screening of combinatorial libraries of new chemical entities

Published on 18 June 2013. Downloaded by University College Cork on 18/06/2013 10:57:28.

and biocatalysts (engineered enzymes with altered catalytic properties).

One well developed area of enzymatic assays is the determination of glucose in biological fluids (blood plasma, urine, saliva, tear, sweat), used in routine clinical tests, diagnostics of human diseases, intensive and personal care (40% of all clinical tests with blood samples include glucose determination[85]), biotechnology. Large clinical analysers, portable devices (glucometers) and specialised systems (*e.g.* implantable biosensors for continuous monitoring, insulin pumps for diabetic care) conduct glucose assays in a number of different formats using enzymatic platforms.

Glucose determination using glucose oxidase and O_2 sensing is well established, solid-state sensors, fibre-optic and soluble probes were applied and demonstrated satisfactory performance.[47,53,72] However, electrochemical and colorimetric biosensors that do not use O_2 detection and optical transduction[19,86] are currently more successful in this huge market than optical biosensor systems because: (1) O_2 transducers operate by measuring a decrease in initially high O_2 concentration ($\sim$200 μM in air-saturated samples[11]) being less sensitive than *e.g.* measurement of H_2O_2 or mediator production;[85] vast excess of ambient O_2 and its diffusion into the sample can also interfere; (2) greater susceptibility of the phosphorescence quenching method to environmental parameters such as temperature, ambient light, oxygenation of blood, sample properties; (3) higher complexity and slower development of optical O_2 transducers compared to their electrochemical and colourimetric counterparts, especially at the start of establishment of this market; (4) non-optimal analytical performance, robustness and costs of early stage optical biosensors. As a result, traditional enzyme biosensors with optical O_2 transducers for glucose and other metabolites have not been very successful so far.

On the other hand, O_2 sensor technology is now more competitive and mature, many high-performance components are available for designing O_2 transducers and biosensors of new generation.[41,43,55] Many of their initial bottlenecks have now been addressed, such that modern phosphorescence based O_2 transducers can now provide: (1) internal referencing and stable calibration through lifetime based O_2 sensing; (2) reliable operation under ambient light conditions and variable sample optical properties; (3) multi-parametric systems with internal compensation for key sample variables, particularly temperature and dissolved O_2; (4) flexible, multi-functional sensor materials compatible with biological samples, affordable and scalable in fabrication; (5) miniaturized, modular and integrated detection architecture; (6) contactless interrogation with the sample, intelligent communication with the detector, software and user/operator (also wireless); (7) improved analytical performance matching or exceeding that of the alternative (*e.g.* electrochemical) biosensors.

A new glucose biosensor uses glucose oxidase, optical O_2 transducer, reference O_2 sensor to correct for dissolved O_2, and a microdialysis unit. Implanted through skin, this microsensor allows long-term transcutaneous measurements of glucose in blood plasma during intensive care, showing advantages over the electrode-based analog.[87] Another recent example is a biosensor for H_2O_2 with Ru-based O_2 transducer and immobilised catalase enzyme.[88]

Significant progress has been achieved with laboratory and screening enzymatic assays which rely on optical O_2 sensing. An important development was their adaptation for standard bioassay substrates, particularly 96- and 384-well microtiter plates, using samples sealed with mineral oil.[89] Also PtCP and PtPFPP based sensors and probes can be used on conventional time-resolved fluorescence readers (originally developed for *in vitro* diagnostic tests using lanthanide chelate labels) without any significant modifications, to perform lifetime-based O_2 sensing by the Rapid Lifetime Determination (RLD) method.[90] In RLD emission intensity signals (F_1, F_2) are collected at two different delay times (t_1, t_2) after the excitation pulse, from which lifetime is calculated as: $\tau = (t_2 - t_1)/\ln(F_1/F_2)$.

Such platforms provide robust, sensitive and simple measurement of enzymatic reactions in complex samples, with a quantitative and accurate readout and stability to optical and quenching interferences.[91] Using automated dispensing and liquid handling (multi-channel pipettes and robotics) and parallel analysis of a large number of samples in kinetic mode (scanning periodically the microplate), a large number of samples can be processed rapidly and conveniently, thus enabling an array of screening applications.[92]

Another significant development has been the high-sensitivity enzymatic assays. In particular, the fluorescence based platform LightCycler® (Roche), dedicated for real-time monitoring of nucleic acid amplification, has been adapted for enzymatic assays with optical O_2 transducers. The glass capillary cuvettes providing a good barrier for ambient O_2 are combined with their efficient temperature control (active ventilation with heated air) and precise mechano-optical alignment in the carousel (accommodates up to 48 samples), provide unsurpassed sensitivity and accuracy in the monitoring of enzymatic O_2 consumption. It has been demonstrated with a number of enzymatic assays of high practical significance, including the detection of monoamine oxidase enzymes, cyclooxygenases, cytochrome P450 isoforms (drug metabolism), their substrates (dopamine and other catecholamines), and inhibitors.[93]

These measurement formats are also applicable to coupled enzymatic reactions. Thus, cholinesterase–choline oxidase system and soluble O_2 probes were used for the detection of cholinesterase inhibitors.[94] These simple and sensitive assay systems operating in the screening format can be used in security and biodefence applications to monitor chemical warfare and relevant toxins.[95] In the coming years, we anticipate a burst of activity in development and application of enzyme biosensors.

4.2. Analysis of mitochondrial respiration

A mitochondrion is a small organelle (size of 0.5–1 μm) present in eukaryotic cells in significant numbers. Mitochondria host the most efficient energy generation pathway, oxidative phosphorylation (OxPhos), and are the main producers of cellular ATP.[5] They consume most of cellular O_2 ($\sim$90%, but may vary for different cell types), while all the other processes utilize the

 This journal is © The Royal Society of Chemistry 2013

Published on 18 June 2013. Downloaded by University College Cork on 18/06/2013 10:57:28.

remaining small portion.[5] Mitochondria participate in many other vital processes within the cell, including Ca^{2+} signalling, ion fluxes, redox homeostasis,[96] generation of reactive oxygen species (ROS) and trans-membrane potentials, initiation of apoptosis and autophagy. They have their own chromosome (mtDNA) encoding some, but not all, of their proteins.[97]

Although tightly connected to the internal cellular life, mitochondria can be isolated from cells and tissues retaining their integrity and many vital functions.[97] They can be manipulated and used to study the complex machinery of the mitochondrion, its diverse range of physiological functions and particularly OxPhos – a multi-enzyme system located in the inner mitochondrial membrane. An essential part of the OxPhos is the Electron Transport Chain (ETC), which consists of complexes I–IV. O_2 molecules act as the terminal acceptor of the ETC at complex IV – cytochrome *c* oxidase. The ETC is largely responsible for the formation and maintenance of physiological gradients of potential, $\Delta\psi_m$, and $[H^+]$, ΔpH_m, across the mitochondrial membrane, producing the proton motive force, pmf, which drives the synthesis of ATP molecules by complex V (ATP-synthase). This is shown schematically in Fig. 5.

As a result, by supplying the different substrates, specific inhibitors of complexes I–V and uncouplers (Fig. 5) and measuring the OCR, one can extract detailed mechanistic information about the activity of different respiration states (states 1–4 respiration[98]), the relative contribution of complex I and complex II pathways, the degree of coupling and spare respiratory capacity upon uncoupling, the mode of action of a drug on the mitochondria and its particular target(s) within. Many other processes linked to or influenced by the OxPhos can also be studied.[97]

Analysis of respiration of isolated mitochondria allows studying of mitochondrial (dys)function, toxicological effects of drugs, detailed bioenergetic and mechanistic studies.[5] Traditionally OCR has been measured in a sealed, stirred chamber with built-in Clark-type O_2 electrode.[97] Although accurate and quantitative, this set-up cannot provide the required throughput and speed (mitochondrial preparations are only stable for a few hours on ice), stability to interferences and reliable measurements at low O_2 levels.

The introduction of quenched phosphorescence O_2 sensing has been an important step forward.[33] Although studied for many decades, many fundamental questions still remain, including the dependence of respiration on O_2 concentration and regulation of OxPhos by internal and external factors. The Oxyphor G2 probe[61] was recently applied to analyse O_2-dependent respiration of mitochondria in a sealed system.[99] K_M for O_2 was shown to decrease significantly at lower pH, an effect which may have physiological consequences giving the advantage to transformed cells over normal cells during cancer progression.

Another milestone was the analysis of mitochondrial respiration in standard microtiter plates using a PtCP based probe MitoXpress®-Xtra (Luxcel Biosciences) on a standard fluorescence plate reader and simple intensity or preferably lifetime based O_2 sensing.[98] Such assays are conducted in partially sealed samples: a layer of mineral oil is applied on top of each sample, thus priming the assay and depletion of O_2 which is then related to the OCR. They currently operate in 96- and 384-well plates, with parallel measurement of samples with different drugs and conditions. Respirometric screening for mitochondrial toxicity is typically performed on two respiration media: one without ADP (state 2 respiration) to identify mitochondrial uncouplers, and another with ADP (state 3 respiration) to identify mitochondrial inhibitors. Inhibition is initially tested at one compound concentration (typically 1 μM), and for positive hits IC50 is subsequently determined. Uncouplers normally

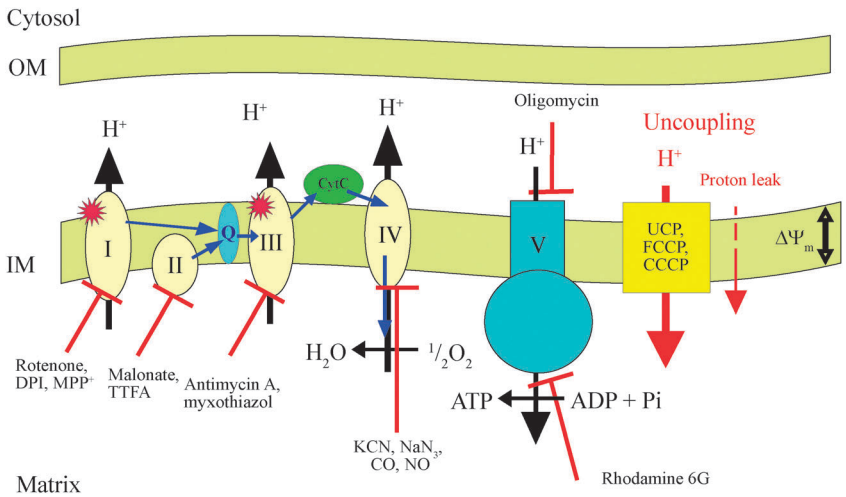

Fig. 5 General representation of OxPhos machinery in the mitochondria of eukaryotes. The ETC consists of four enzymes: complexes I (NADH-ubiquinol-oxidoreductase), II (succinate-ubiquinol oxidoreductase), III (ubiquinol-cytochrome *c* oxidoreductase) and IV (cytochrome *c* oxidase) located in the inner mitochondrial membrane.[97] Transfer of electrons (blue arrows) is mediated by coenzyme Q_{10} (Q) and cytochrome *c* (cyt *c*) and results in O_2 consumption at complex IV. The proton, ΔpH_m, and potential, $\Delta\psi_m$, gradients are used to produce ATP by complex V (F_0F_1 ATP-synthase). Electron leaks at complexes I and III (indicated by stars) generate superoxide radical ($^{\bullet}O_2^-$) – the main source of ROS. Proton movement across the inner membrane is possible through the action of protonophores (FCCP, CCCP), uncoupling proteins (UCP) or intrinsic proton leak. Mitochondrial function is also linked to Krebs cycle (supplies succinate), Ca^{2+} signalling, apoptosis and other cellular processes.[97] OM – outer mitochondrial membrane, IM – inner mitochondrial membrane.

Published on 18 June 2013. Downloaded by University College Cork on 18/06/2013 10:57:28.

produce bell-shaped responses (increased respiration due to uncoupling followed by decrease due to toxicity), and to avoid false-negative results they must be tested at several different concentrations. This method has been adopted by pharmaceutical companies as a screen for mitochondrial toxicity of drug candidates.[89,98]

Multi-parametric assessment of mitochondrial function of animal tissue and organs was also undertaken by combined measurement of OCR with MitoXpress®-Xtra probe and mitochondrial swelling, membrane potential and cytochrome *c* release, which provided mechanistic information on drug induced injury of liver tissue.[100] Solid-state sensor systems including coated microplates[101] and a Seahorse XF analyser (see Section 4.3) were also used in this application.[102]

At the same time, analysis of isolated mitochondria has a number of limitations, mainly the lack of relevance to the context of the whole cell. For drugs that cannot easily pass cell membranes and reach mitochondrial components the observed effects appear to be overestimated. Many drugs with specific transport mechanisms, tissue specificity, metabolism inside the cell or effects on other metabolic pathways are difficult to study. The results are also influenced by the isolation procedure which determines the degree of 'coupling' and quality of mitochondrial preparations. Many of these issues can be overcome by analysing whole cells.

4.3. Mammalian cell respiration

Mammalian cell cultures are in the centre of life sciences and biomedical research. They allow researchers to study cellular processes in their integrity and conditions resembling the physiological environment (adherent state, contacts with neighbouring cells). Respiration of intact cells accounts for transport of key nutrients including O_2, the multiple regulatory networks and compensatory mechanisms, other energy generating, metabolic and signalling pathways and secondary factors acting in the cells. Non-mitochondrial O_2 consumption can also be probed.

General strategies for microplate based OCR measurements with cells are similar to those described in Sections 4.1 and 4.2. However, weak respiration of mammalian cells (<1 nM O_2 per min per 10^6 cells[5]) is more difficult to measure, especially for adherent cells the maximal density of which is limited by the confluent layer. Low respiration rates and back-diffusion of atmospheric O_2 make determination of absolute OCRs more difficult, however relative changes in OCR can be measured reliably. So far, many types of mammalian cells including liver, muscle, neuronal cell lines, primary cells and induced pluripotent stem cells were measured in standard microplates with samples sealed with mineral oil[89] and detection on a standard fluorescence reader.[98,103,104] Moreover, photophysical characteristics of a MitoXpress®-Xtra probe allow multiplexing with a long-decay pH-sensitive lanthanide probe pH-Xtra™ (Luxcel Biosciences), and parallel measurement of OCR and extracellular acidification (ECA) in the same sample without cross-talk.[104] Other fluorescent probes and cell-based assays can be added in the multiplex or parallel format.

Seahorse Bioscience designed an integrated opto-mechanical system for OCR and ECA measurements with adherent cells, called an XF analyser. It operates with dedicated microplates having specially shaped wells and moving cartridges with solid-state phosphorescent O_2 and pH sensors and light guides.[105] During the measurement cycle, the cartridges create micro-chambers at the bottom of each well sealing the cells and providing rapid and sensitive quantification of OCR and ECA (due to a high cell volume to sample volume ratio). Complex modelling is used to compensate for O_2 leaks and work out absolute OCR values for the respiring sample.[106] The analyser exists in 24 and 96-well plate modifications, with two or three-parametric (with CO_2 sensors) detection, built-in thermostats, drug vessels and injectors for each well. This system has been used with many different cell lines, primary cells and β-cell islets and also with suspension cells and isolated mitochondria where its benefits are not so evident.[96,105]

The above two platforms enable the simultaneous assessment of the two main energy production pathways within the cells: OxPhos (OCR) and glycolysis (ECA). Further multiplexing can be applied in the analysis of drug-induced toxicity, mitochondrial (dys)function, disease models, ageing, biotechnology and many therapeutic areas.[107,108]

4.3.1. Analysis of drug-induced toxicity. Different transport, degradation and action mechanisms for a drug in isolated mitochondria and in intact cells often result in different patterns of toxicity. Consequently, organ toxicity and drug safety assessment is now shifting towards cell-based models. OCR assays can provide valuable information about the mode of drug action and possible toxicological effects *in vivo*,[109,110] especially when bundled together with other markers of toxicity.

Examples of action of different model drugs on cells and prognostic values of different biomarkers are shown in Fig. 6. Thus, total cellular ATP assay, which provides information on general viability and non-specific cytotoxicity, misses many toxins with strong effects on cell metabolism and bioenergetics. OCR is much more sensitive and selective identifying both uncouplers (FCCP) and inhibitors (antimycin, rotenone) of respiration. For drugs that act on the glycolytic ATP pathway (okadaic acid), changes in OCR may not be so prominent, but clearly detectable by combined OCR/ECA assay.[97]

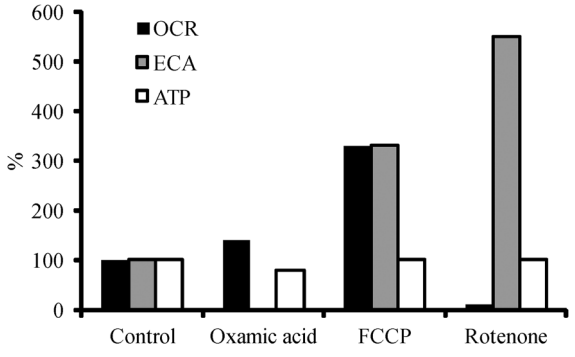

Fig. 6 Responses of drugs with different mode of action on cell metabolism assessed by the ATP, OCR and ECA assays. Modified from ref. 104.

This journal is © The Royal Society of Chemistry 2013

Published on 18 June 2013. Downloaded by University College Cork on 18/06/2013 10:57:28.

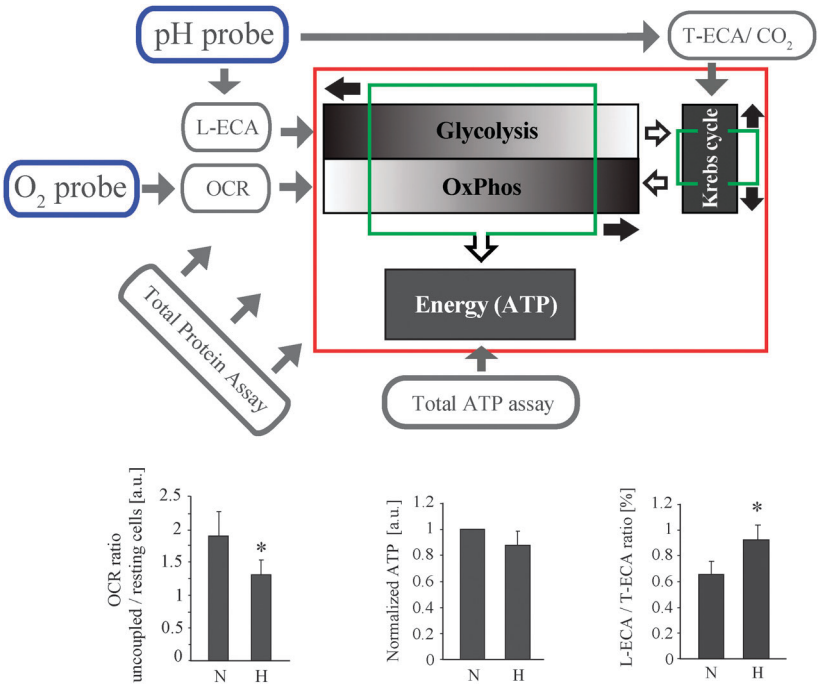

Fig. 7 Representation of the main cell energy generating pathways of the cell and CEB concept. Normal balance of glycolysis, OxPhos and Krebs cycle (green rectangles) can be perturbed by mutations, drugs, or other factors. The balance of different pathways can be probed using indicated methods: OxPhos/OCR – with an O_2 probe in sealed samples; glycolysis/L-ECA (lactate component) – with a pH probe in unsealed samples; Krebs cycle/T-ECA (total – lactate and CO_2) – with a pH probe in sealed samples; total ATP/general cell viability – with a commercial bioluminescent kit; variation of biomass in different samples – with total protein assay (modified from ref. 114). Bottom panel: demonstration of CEB with neural PC12 cells maintained under 21% (normoxia, N) and 3% O_2 for 30 days (hypoxia, H). Altered OCR, ATP and L-ECA/T-ECA ratios reflect a reduction in OxPhos, increase in glycolytic flux in H-cells and reduced spare capacity (modified from ref. 117).

A two-parametric OCR/ECA platform for cell-based screening of drug-induced mitochondrial dysfunction and organ toxicity using a MitoXpress®-Xtra probe and standard 384-well plates was developed and validated with 200 commercial compounds on a common suspension cell line, HL60.[103] Similar tests can be carried out on an XF analyzer.[111] The two systems show comparable data, XF is a standalone unit with dedicated consumables for enhanced sensitivity, whereas the MitoXpress® platform operating on standard microplates and plate readers targets flexibility, high throughput and low cost.

Multi-parametric analysis of respiration and other markers revealed new targets for another pharmacological agent – bafilomycin A1, a commonly used inhibitor of V-ATPase and potential anti-cancer drug[112] (see Section 4.5). In addition to V-ATPase inhibition, bafilomycin was shown to enhance OCR through mild mitochondrial uncoupling in neuronal cells.

A mechanistic toxicological study was described with microcystins, hepatotoxins produced by cyanobacteria during algal blooms which can contaminate fresh and drinking water. Microcystins are taken up by liver cells *via* organic anion transporting polypeptides (OATP) and inhibit cellular protein phosphatases inducing toxic effects. The study with microcystin-LR and measurement of OCR, ROS, cellular ATP, ECA and phosphatase activity in different cell lines and primary hepatocytes revealed new targets for microcystins in the mitochondria and an uncoupling effect on respiration.[113] Furthermore, a new screening test for the presence of microcystins in environmental samples was developed, which uses ordinary cell lines (normally immune to microcystins as they lack OATP) and facilitated delivery of the toxin with the aid of transfection reagent. Showing sub-nM sensitivity, this *in vitro* test offers a viable alternative to current tests for microcystins on animals and primary hepatocytes, or by ELISA.

4.3.2. Assessment of cell bioenergetics. The above platforms based on optical O_2 and pH probes/sensors can be incorporated into a larger suite of assays to provide comprehensive assessment of cell bioenergetics and related processes. Plate reader platforms are particularly amenable to multi-parametric analysis, one such concept called 'Cell Energy Budget' (CEB) is presented schematically in Fig. 7.

According to CEB, OCR/ECA assays (see Section 4.3.1) were extended with ECA measurement in sealed (T-ECA) and unsealed (L-ECA) samples. This allowed an assessment of the individual contribution of anaerobic glycolysis (produces lactate which is extruded from the cells) and Krebs cycle (produces CO_2 which remains in sealed samples but escapes from unsealed). Total ATP assay was introduced to monitor overall cell viability (energy depletion and death), and total protein assay – to correct for differences in biomass (cell number, size, growth rate) in different samples. Furthermore, the cells are measured both in resting and uncoupled (with FCCP added) states, thus determining basal and maximal respiration and glycolytic fluxes (*i.e.* spare capacity).

A typical CEB experiment includes: (1) kinetic OCR assay with O_2 probe (MitoXpress®-Xtra) and sealed samples to measure

Published on 18 June 2013. Downloaded by University College Cork on 18/06/2013 10:57:28.

basal and maximal respiration; (2) kinetic L-ECA assay with pH probe (pH-Xtra) and unsealed samples to measure glycolytic flux; (3) kinetic T-ECA assay with pH probe (pH-Xtra) and sealed sample to determine Krebs cycle activity as the difference between T-ECA and L-ECA; (4) end-point measurement of total cellular ATP with a luminescent kit, and (5) total protein assay followed by normalisation of measured OCR, ECA and ATP values for biomass content. Each assay is performed in several replicates (3–5), providing statistically plausible data.

In this form, CEB provides a powerful tool for the analysis of different cells (normal, diseased, treated, transformed or different types), their metabolic features and modulators of cell bioenergetics and mitochondrial function.[114] It minimises the risk of missing minor impairments in key pathways due to compensation by alternative pathways. Such 'masking' can occur in the basal, but not the uncoupled state. Similar studies can also be performed on Seahorse XF analyser, the new model of which also measures O_2, pH and CO_2.

The CEB concept was applied for analysis of mitochondrial protein PNC1 which is involved in mtDNA biogenesis,[114,115] Krebs cycle enzyme fumarate hydratase implicated in renal cell cancer and hereditary leiomyomatosis[114,116] and the effect of long-term hypoxia (physiological normoxia) on the function of neural cancer cells.[117]

Simple OCR measurements were also applied in many physiological studies. Thus, increased biogenesis and PGC-1α levels were seen to increase O_2 consumption leading to sustained hypoxia and stabilisation of HIF-1α protein, thus proving that PGC-1α and HIF-1α pathways are cross-regulated.[118] Studies on cancer metabolism,[119–121] mitochondrial dysfunction due to loss of function of cellular proteins,[115,116,122,123] hypoxia,[117] differentiation and function of osteoclast cells in rheumatoid arthritis,[124] function of primary[125] and stem cells,[126] ageing[127] were also studied using this method.

Overall, OCR assays with mammalian cell models can be used to study general mechanisms of aerobic respiration, ROS, NO and Ca^{2+} signalling, uncoupling proteins, thermoregulation and obesity, neurodegeneration, cardiovascular and metabolic diseases, hypoxia research. Also drug discovery and development are now shifting from relatively non-specific 'gunshot' screening of compound libraries on cell models to more focused approaches which provide mechanistic information and quantitative structure–activity relationships (SARs) about particular targets, metabolic pathways and signalling networks in the cell and whole tissue. The basic panel can be expanded and customised with other functional assays. In this regard, respirometric cell-based assays and the CEB platform provide powerful tools. Another important area is security and biodefence, where such cell-based assay platforms can be used to detect low toxins, chemical and biological warfare at low levels, with high sensitivity and selectivity.

At the same time, traditional 2D cell cultures also possess drawbacks, the main being their limited resemblance of 3D environment in live tissue and organs. Replacement of cell monolayers and detached cells with mixed cultures, 3D scaffold and spheroid models, tissue slices, and the use of microfluidic biochips and *ex vivo* models[128] can address this (see Sections 4.6–4.8).

4.4. O_2 in microbial cultures

Microbiology deals with a broad range of microorganisms from viruses to fungi. Some of these are pathogenic and possess significant hazard to human health, for example, deadly infections, food borne (*E. coli* O157), clinical (MRSA, rotavirus) and environmental (*Campylobacter*, coliforms) pathogens. These have to be monitored at very low concentrations, down to one viable cell, prevented from uncontrolled circulation and proliferation, and eradicated if possible. Other microorganisms are very beneficial for mankind, actively used in human practice (baker yeasts, lactic bacteria) and biotechnology (microbial fermentations, production and degradation of biopolymers, drugs), or being inherent part of our body (*e.g.* microflora in the gut, skin). Viruses do not have their own metabolism and utilise infected cells for replication, however their invasion changes homeostatic and functional conditions of host cells and this can be used for indirect detection *via* O_2.

Aerobic and microaerobic bacteria consume significant amounts of O_2, and therefore are dependent on aeration conditions. Compared to mammalian cells, common aerobic bacteria are characterised by high proliferation rates (typical doubling times >24 h and <30 min, respectively) and respiration.[129] At the same time, bacterial cultures exhibit different growth phases: lag phase, exponential growth, stationary (substrate limitation) and death (depletion of nutrients) phases,[130] and are able to quickly adjust their metabolism to new environmental conditions, nutrients and O_2 availability, stress factors. Stressed or injured bacteria (*e.g.* after dehydration, sterilisation or drug treatment) can stay in the lag phase for a long time before they enter active growth and respiration. Such behaviour makes their detection *via* O_2 respiration more difficult. Nonetheless, when placed in a nutrient-rich media which promotes growth, microbial samples can quickly enter exponential growth and produce a robust change in oxygenation conditions. The change, which usually occurs at a point when critical cell numbers and OCR are reached, is easily detectable using an O_2 sensor.

Respirometric analyses of bacterial cultures by quenched-phosphorescence O_2 sensing[131,132] are gaining popularity. Dedicated products such as BD Biosensor™ plates (Becton Dickinson), SensorDish® Reader and plates (Presens), the vial and plate based systems GreenLight® 910, 930 and 960 (Mocon-Luxcel Biosciences partnership)[133,134] are commercially available. They allow rapid, high throughput analysis of microbial cultures and complex samples, high sensitivity (down to a single viable cell), broad dynamic range (10^0–10^8 cfu ml^{-1}), simple add and measure procedure, general convenience, affordable costs and broad range of applications. Therefore micro-respirometry in *liquid* media provides an attractive alternative to the conventional colony counting method on solid media (agar plating[135]) and other rapid microbiological methods.[136] O_2 profiles can be used to determine the absence (sterility) or the presence of *viable* aerobic microorganisms, their proliferation rate and metabolic activity. Enumeration of bacteria in original samples can be achieved by applying pre-determined analytical relationship (calibration) to respirometric data. Doubling times can be

 This journal is © The Royal Society of Chemistry 2013

Published on 18 June 2013. Downloaded by University College Cork on 18/06/2013 10:57:28.

determined by analysing the sample at two or more dilutions, and used for predictive identification of microbial species.[137] Yeast and fungi are also detectable using this method, though their respiration can be significantly slower than for bacteria.[138]

Metabolic and chemical interactions between different organisms is an emerging area, for example in gut health, (neuro)gastroenterology, studies of biogeochemical communities in soil.[2] Secondary metabolites often possess the functions of antibiotics, toxins, elicitors or signals in such systems.[10] Antifungal bacterial metabolite 1,4-diacetylphloroglucinol was studied in cultures of *S. cerevisiae* by high-throughput OCR measurements, uncovering its new uncoupling effect on yeast mitochondria.[139]

Detection of intrinsic bioluminescence of *Vibrio fischeri* bacteria (*e.g.* Microtox® kits) is currently used as a standard acute toxicity testing method for chemical and environmental samples.[140] Being relatively fast, sensitive and simple, this test is limited to one particular organism (prokaryote), problematic with samples that are turbid, absorb light, quench or interfere with the luminescent reaction, and operates on a dedicated instrument. An alternative approach has been proposed based on respirometric detection with MitoXpress®-Xtra probe in standard microplates on a fluorescent plate reader.[141] Using a similar procedure to the MicroTox, this respirometric test produces comparable results with *V. fischeri*, but improved sample throughput, automation and miniaturization. It is not limited to luminescent bacterial strains, and can use many other test organisms and their panels which may include prokaryotic and eukaryotic cells, small invertebrates and vertebrates.[142] Such 'respirometric profiling' provides more detailed toxicological data and can be used for predictive identification of different groups of toxicants.

As growth and respiration depend on the culturing conditions (media, temperature, pH, ions, additives),[143] selective determination of particular microbial species and genera can be achieved using appropriate media and condition. However, the diversity of bacterial species and strains having similar metabolic and growth patterns and complex mixtures present in real samples limit the potential of their definitive selective determination (other microbiological methods face the same challenges). Also when a mixture of different bacteria is placed in growth promoting medium, faster growing and more robust species can overgrow the others and 'mask' their respiration.

Nonetheless, in a recent study, a panel of 9 common species of aerobic bacteria was investigated by high-throughput micro-respirometry in 384-well plates with 16 partially selective media.[137] For each medium and bacterial strain, growth profiles were recorded at different dilutions, and standard curves, doubling times and growth patterns in different media determined. Selective, sensitive and rapid (one day experiment) determination of bacteria in pure cultures and simple mixtures was thus demonstrated as a proof of concept. Existing selective tests with other transducers (*e.g.* Biolumix system with colorimetric pH/CO_2 sensors[144]), can be adapted for O_2 sensing, bringing additional benefits.

For comparison, a standard selective microbiological test (ISO method 07.100.30, 4831–4833) usually involves: (1) pre-enrichment (24 h) to resuscitate stressed bacteria and encourage their growth; (2) selective enrichment (24–48 h) to increase target pathogen numbers to detectable levels and suppress non-target cells; (3) selective and differential plating (24–48 h) on chromogenic agar to identify pathogens of interest; (4) confirmation by biochemical or serological identification. Definitive identification of bacterial strains (*E. coli* O157 and alike) can also be achieved by the molecular methods (immunological and nucleic acid tests), but these require skilled personnel, special equipment, and have higher costs.

Similar to the cell-based assays (see Section 4.4), the respirometric microbial assays also allow multiplexing with other tests. For example, they can be used as part of the pre-enrichment and/or selective enrichment steps, to identify negative samples and exclude them from further testing, or combined with traditional tests with chromogenic metabolic substrates.[137] Coupling with optical sensors for pH, CO_2 or ammonia, which operate in a similar format as the O_2 sensor[104] can also improve the selectivity of such microbial assays.

Unicellular bacteria can form or be incorporated into organised aggregate structures – biofilms. Microbial biofilms secrete substances supporting their growth, similar to an extracellular matrix in mammalian tissue. Functional properties of microbial cells in the dispersed state and in biofilms are different, and this knowledge is important for many other areas particularly infectious diseases. *Pseudomonas aeruginosa*, a facultative anaerobic bacterium with reduced growth and metabolic activity at low O_2 levels, is almost inescapable in patients with cystic fibrosis and impaired lung function. Creating hypoxic regions in tissue, it survives antibiotic treatments (*e.g.* tobramycin, ciprofloxacin, and tetracycline) which preferentially kill the physiologically active bacteria living at high oxygen levels.[145] Using O_2 sensing and imaging, *P. aeruginosa* films were investigated as a model of infections in cystic fibrosis.[146,147] O_2 dynamics was also studied in *Staphylococcus aureus* biofilms by ratiometric measurements of 1 μm silica particles with ruthenium and Nile blue dye, and showed a significant role in organ transplantation, also increased antibiotic resistance.[148]

Other applications of microbial micro-respirometry include screening for antimicrobial drugs and drug resistance, development of new growth media (especially selective media for particular pathogens); development and combinatorial testing of nutraceuticals and probiotics (beneficial for human and animal health by promoting microflora and improving healthy living), optimisation and control of treatment methods (processing, sterilisation, preservation) for food, pharmaceutical, environmental and clinical samples, beverages and microbial cultures (see below).

4.5. Food and microbial safety

Food and other perishable products usually degrade rapidly under high O_2 conditions, through oxidation (of lipids, destruction of ascorbic acid), enzymatic reactions (fast ripening, browning of fruit and vegetables), and microbial spoilage by bacteria, yeast and fungi many of which are active consumers of O_2.[149] Microbial spoilage and contamination with common food borne pathogens is of major concern for the food, packaging and retail industries,

Published on 18 June 2013. Downloaded by University College Cork on 18/06/2013 10:57:28.

customers and society in general. The following pathogens are specifically cited by the legislation: *Listeria monocytogenes*, *Salmonella* spp. (including typhimurium and enteritidis), *E. coli* (indicator of faecal contamination), *Enterobacteriaceae*, *Staphylococci*, *Bacillus cereus*, and zero tolerance limits have been established for some of them.[150] Packaging under modified atmosphere (MAP) with low O_2 is therefore used for many foods. In this context, O_2 levels and dynamics in food packs are important indicators of quality, safety and microbial load of food products.[151] Optical O_2 sensing can greatly facilitate such monitoring.

Non-destructive monitoring of O_2 in packs is achieved by incorporating phosphorescent sensors either directly at the packaging line (inserts, stickers, labels[149,152,153]) or using pre-made packaging materials integrated with sensors. Such 'smart' packs can be interrogated using an optical scanner which reads sensor signals and determines O_2 concentration. Disposable, low-cost solid-state sensors made from food-compatible materials (polymeric composites) are the preferred format for this application. Temperature of the pack also needs to be measured, *e.g.* using a contactless IR temperature sensor, which is used for correction of optical readings. Measurements in many packs (having different and variable shapes and sizes) can be conducted with one instrument in a high throughput manner, repetitively and without affecting package integrity. This approach has proven its utility for quality and safety assessment of packaged products, including modified atmosphere packaged meats, fish, cheese,[154] green produce, ready-to-eat foods.[153,155] Solid-state O_2 sensors were also used with beverages to control beer brewing,[156] quality and sensory characteristics of pre- and post-pasteurized lager.[157] These sensor systems enable the identification of faulty packs, problems with packaging materials and processes, manufacturing, storage and transportation issues, batch testing and shelf life studies with a large number of packs.[149,152] Commercial systems for such applications include Optech® Platinum (Mocon-Luxcel), Fibox 3 (PreSens, Germany), OxySense Oxygen Analysers (OxySense, USA), FirestingO2 (Pyro Sciences, Germany). Colorimetric O_2 sensors and 'consume within' indicators[149] derived from them have been developed (Embedded Timer™, Insignia Technologies), which also have significant potential for food and consumer safety.

Non-destructive assessment of microbial load and growth in food packs is also possible, but has its limitations. Enzymatic and chemical (by scavengers) consumption of O_2, intrinsic respiration of food products (green produce, vegetables), diffusion of atmospheric O_2 across packaging material, volume of headspace should all be taken into consideration as they also affect residual O_2 levels. Due to low O_2, high CO_2 and antimicrobial preservatives in packaged food products, monitoring of microbial respiration is difficult and may result in poor predictability of the actual microbial load and related hazard. Microbial growth on the surface of the product may lead to variability of results. On the other hand, for products packaged at moderate O_2 levels (convenience foods, green produce), residual O_2 levels in sealed packs showed clear correlation with their microbial load and dynamics under different packaging and storage conditions.[149] Knowing these relationships, non-destructive measurements with a phosphorescent O_2 sensor can be used for assessment of particular products.

However, analysis of microbial safety of foods using sampling methods[158] is much more efficient (though destructive). It allows for more optimal conditions for respirometric measurements: (1) homogenisation of food samples and addition of nutrient-rich media (usually 1 : 10 w/w) eliminate stress conditions in the pack and promote fast microbial growth; (2) respirometric assay is performed with air-saturated samples (diluted with medium) and at optimal temperature (*e.g.* 30 °C or 37 °C); (3) monitoring of O_2 depletion in *liquid* medium under seal (*i.e.* without headspace). All this ensures rapid, sensitive, reproducible and robust assay with crude food homogenates, with smooth respiration profiles, and accurate determination of microbial load (Total Viable Counts, TVCs).

Such respirometric TVC assays are performed in microtiter plates[132,158] or disposable vials at constant temperature (30 °C), on a phosphorescent reader which determines the onset/threshold time (TT) of the probe/sensor signal for each sample. TT is the time from the start of the experiment when the phosphorescent signal increases above the basal (air-saturated) level and reaches the pre-set threshold level. TT usually produces a linear relationship with the logarithm of microbial load in the original sample, log(cfu/ml), making it a convenient parameter for quantification. Samples with higher TVCs produce shorter TT values (reciprocal relationship), so that highly contaminated samples can be identified within a few hours in real time. Representative oxygenation profiles (raw data) produced by samples containing aerobic bacteria and processed results are presented in Fig. 8.

The respirometric platform for rapid TVC tests has been shown to work reliably with complex and coloured samples, crude homogenates and different food matrices.[158] It is more stable and robust than alternative turbidimetry (absorbance at 600 nm), bioluminescence (total ATP) or flow cytometry methods.[159] For industrial applications, it is currently provided in several configurations: (1) a high-throughput GreenLight® 960 system which uses a soluble O_2 probe, 96/384 well plates and measurement of samples sealed under oil on a standard TR-F plate reader; (2) a medium-throughput GreenLight® 930 system operating with disposable plastic vials (2 mL volume, bar-coded) with built-in sensors, and an automated carousel detector/incubator which accommodates up to 48 vials, provides TVC quantification and classification of test samples in real-time; (3) a low-throughput GreenLight® 910 system, a simplified version of the 930 system which measures one vial at a time manually. The GreenLight® tests (marketed by Mocon and Luxcel Biosciences) have been certified by AOAC/MicroVal for food safety applications – determination of TVCs in raw meat and other products (AOAC licence no. 061002). Such testing can be combined with other quality testing methods used by the industry, including the non-destructive sensing of O_2 and CO_2 in packages. This has been demonstrated with packaged ready to eat salads,[153] raw fish and some other food products.[153,154,160]

An ultra-high throughput imaging system was developed by Techno-Path for testing of raw and processed milk. It uses microplates with phosphorescent sensors, operates in a simple

 This journal is © The Royal Society of Chemistry 2013

Published on 18 June 2013. Downloaded by University College Cork on 18/06/2013 10:57:28.

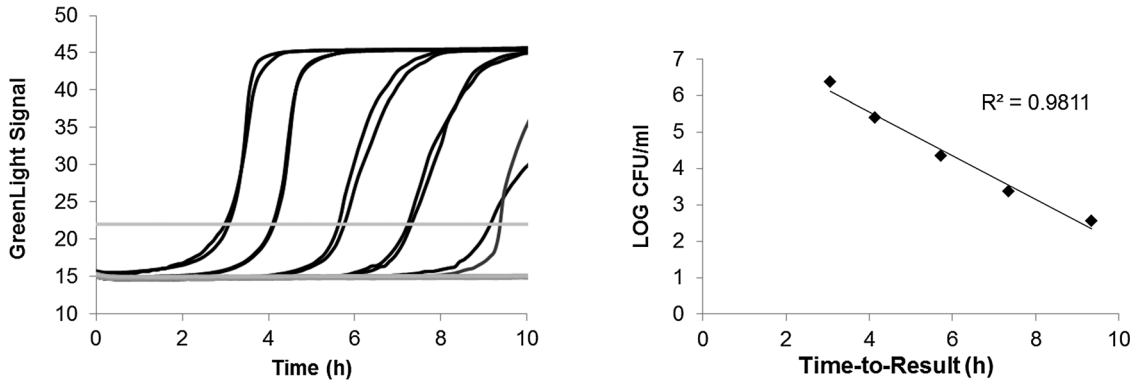

Fig. 8 Oxygenation profiles (left) of food samples spiked with different concentrations of *Bacillus cereus* and the resulting calibration (right). Threshold and air-saturated signal levels (phosphorescence lifetime) are shown with grey lines. Samples were measured on GreenLight® platform at 30 °C in duplicates (courtesy of Luxcel Biosciences).

'mix and measure' procedure and can process up to 1000 samples per day.

Theoretical and practical sensitivity of respirometric microbial assays is one viable cell per sample measured.[158] For 96-well plates with 0.1 mL samples diluted 1 : 10 during homogenisation, statistically reliable detection of microbial load in food specimens is 10^2–10^3 cfu g^{-1} and higher. For assays in higher sample volume the sensitivity increases proportionally: for GreenLight® 930/910 systems working with 2 mL and 15 mL vials, the limits of detection are approximately 50 and 7 cfu g^{-1}. For homogeneous liquid samples, dilution can be reduced by adding concentrated medium or nutrients directly into the sample, thus improving the sensitivity 10-fold.

High sensitivity, flexibility and other useful features of the respirometric microbial testing make it attractive for other biodetection applications. Thus, surface swabs can be analysed in larger vials and used for hygiene monitoring at workplaces. Detection of microbial warfare (directly or after retention and concentration on air or liquid filters), coliforms in freshwater and groundwater (require sensitivity at 1 cell in a 100 mL sample), Biological Oxygen Demand,[161] analysis of wastewater and environmental samples can be conducted. Monitoring systems to protect from terrorist attacks with biological weapons and to detect biological warfare can also be developed.

There is a potential to adapt these platforms for *selective* determination of microbial pathogens in food. As outlined in Section 4.4, such assays still require improvement of selectivity and adaptation to 'real life' conditions and complex samples. Active microbiological research on characteristic metabolic features of common pathogens,[139] rational design and high-throughput optimisation of new selective media are expected to accelerate this work and bring to use selective respirometric tests for common food borne pathogens.

4.6. Control of cell oxygenation and O_2 gradients in cell cultures

Since Lavoisier's discovery of toxic effects of high O_2 concentrations, numerous studies have been conducted on animals and cell models.[162,163] At the cellular level, elevated O_2 was shown to have mutagenic and apoptotic effects, promote tumorigenesis,[164–168] and affect senescence and proliferation.[169] However, most of routine cell culture is still performed at ambient O_2 (5% CO_2, 19% O_2, 76% N_2), *i.e.* several times higher than physiological normoxia in mammalian tissue. This mismatch imposes stress on the cells through increased ROS generation, reduced levels of antioxidants,[170] altered metabolism and bioenergetics (generation of highly glycolytic cancer cell lines, the Warburg effect, cell transformation – see Section 4.3).

Researchers are now switching to tissue culture in workstations operating at low O_2, special hypoxia chambers and instruments with built-in atmospheric control (*e.g.* plate readers, microscopes). Although more physiological, these systems usually control atmospheric O_2 levels, but not within samples where respiring cells consume O_2 in the surrounding media and act as O_2 sinks. Significant *local* O_2 gradients have been reported for adherent cells grown at 21% O_2,[171] and they are more prominent at low O_2 and in larger objects such as 3D spheroids and tissue slices.[128,172] Micro-gradients can be eliminated by continuous perfusion, rigorous stirring or shaking, culturing cells on gas-permeable membranes facilitating mass exchange,[173] however this is not always applicable. Reliable *in situ* control of cell oxygenation is highly needed, especially for static cell cultures in flasks and microplates, and this can be achieved with appropriate O_2 probes and sensors.

Extracellular probes are not so efficient, as they get distributed in bulk sample and provide information on average oxygenation.[174] Sensor coatings also have biocompatibility issues so that adherent cells usually grow around the sensor but not on it. Microsensors require micromanipulators to bring them to the cell layer, their fragility and point measurements are significant limitations. On the other hand, cell-penetrating O_2 probes have been successful in providing reliable, accurate and minimally invasive monitoring of oxygenation of cells with minimal toxicity impact on cellular function.[171] This application imposes special requirements on the probe, cell loading and measurement strategies, which have been addressed through intensive research. A number of approaches are described here.

Phagocytic cells such as macrophages are known for their ability to ingest particulate matter. This can be exploited with

Published on 18 June 2013. Downloaded by University College Cork on 18/06/2013 10:57:28.

micro- and nano-particle probes which have no or little intrinsic ability to penetrate cells. Phosphorescent nanoparticles (40 nm Pt-Fluospheres, Invitrogen) were used to measure changes in O_2 during phagocytosis of bacteria,[175] revealing a coordinated inflammatory response of macrophage populations to the invading pathogens. Polystyrene microspheres consumed by RAW264.7 macrophages were used to measure oxygenation and OCR of an individual cell in a microchamber device on a FLIM microscope with gated CCD camera.[176] Although working with phagocytic cells, such loading has moderate/low efficiency, and requires high concentrations (>100 μg ml^{-1}) stressing the cells.

For non-phagocytic cells more sophisticated loading strategies are required. Microinjection, gene gun,[68,177] partial cell permeabilisation (with Ru-dye introduced in esophageal epithelial cells[178]) and electroporation have been tested, but these techniques are invasive, damaging to the cell and rather inefficient. Facilitated delivery with transfection reagent (MitoXpress®-Xtra probe and EndoPorter®, respectively) was a significant improvement,[91] however this method is rather slow (loading times 24–28 h), and has moderate efficiency and cell-specificity so that some cell types cannot be loaded and analysed. The new generation of cell-penetrating small molecule and nanoparticle-based probes[18] has greatly improved the situation.

Traditional O_2 sensing materials usually have low intrinsic ability to enter the cells, localise in a predictable manner and stay inside for sufficient time permitting optical measurements without causing significant cyto- and phototoxic insult.[179] Anionic polycarboxylic porphyrins show weak penetration across the cell membrane which bears a negative charge. Hydrophobic dyes have poor solubility in water, bind non-specifically to and migrate across various biological structures and surfaces. Other dyes do penetrate into the cell, but often show toxicity, probably due to membrane or nuclear localisation and interaction with DNA (*e.g.* cationic porphyrins, Ir- and Ru-dyes[179,180]). Hence, significant tuning of physical–chemical properties of the phosphorescent structures (hydrophilicity, water solubility, charges, special functional groups) and introduction of a suitable 'delivery vector' are usually required. This can be achieved by rational chemical design based on the knowledge of intracellular transport and trafficking mechanisms for different chemical moieties, development of new dyes and delivery strategies, rigorous experimental testing and optimisation with different cell types or more complex models. A number of such probe structures and studies have been performed in recent years (reviewed in ref. 18). Currently, the core–shell polymeric and cationic nanoparticles impregnated with hydrophobic dyes, and conjugates of hydrophilic Pd and Pt-porphyrin derivatives with peptides and other vectors[181–183] are the most efficient for loading and sensing O_2 in mammalian cells. Several key factors determine cell loading efficiency: probe concentration, loading time and conditions (temperature, media, additives), mechanism(s) of transport (cell specificity), migration and leakage from the cell, specific brightness and photostability, cytotoxicity and photo-induced toxicity.[70,181] These parameters need to be carefully investigated for each probe and optimised for the measurements.

The probes such as MitoXpress®-Intra, MitoImage™-NanO2 and MitoImage™-MM2 (Luxcel Biosciences), provide efficient passive loading of cells by simply adding them to the medium at low μg ml^{-1} concentrations, 6–16 h incubation, and subsequent analysis of cells by phosphorescence quenching.[181,184] Similar to the extracellular probes and sensors used in OCR measurements and micro-respirometry (see Sections 4.1–4.3), cell-penetrating probes based on PtPFPP and PtCP dyes are compatible with available detection instrumentation and can be measured on standard TR-F readers supporting the RLD mode to analyse O_2 in cell populations.[91] Residing in the cell, they can provide information on cellular hypoxia at different times and conditions, and allow manipulation (washing and treatment of cells) and long-term experiments.[18] Other indicator dyes, including the short-decay ruthenium complexes and longwave PtTBP and PdTCPP dyes, are not so compatible with such readers, which rely on xenon flash-lamp excitation (not suitable for detection of lifetimes <10 μs) and PMT detectors (poor sensitivity at wavelengths >700 nm), however instrumentation development is expected to improve the situation.[45]

A new real-time method for measurement of oxygenation of cells and their responses to metabolic stimulation was developed recently which is carried out in an open plate (unsealed samples exposed to the atmosphere).[91] Under static conditions, oxygenation of the cell layer is a function of OCR, hence this can be used to trace and quantify changes in cell respiration. A number of sample parameters also affect the oxygenation, including atmospheric pO_2, height and viscosity of the medium layer (diffusion barrier for ambient O_2), temperature, and sample geometry. However, these parameters are easy to keep constant or use them to make the optical response more easy to detect.[171] In this high-throughput metabolic assay, pre-treatment of cells and multiple additions of effectors (small aliquots of drugs) during the monitoring are possible, as shown in Fig. 9.

The cell-permeable and biocompatible O_2 probes with enhanced photostability, brightness, reference and light antenna moieties for multi-modal detection (*e.g.* MitoImage™ NanO2, MitoImage™ MM2 and some others[18]) have enabled O_2 analyses on live-cell fluorescence imaging and high-content screening platforms, on a scale of a single cell. High-resolution O_2 imaging facilitates the analysis of heterogeneous samples,

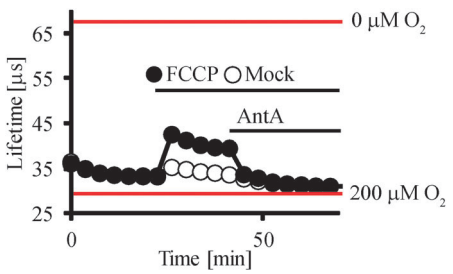

Fig. 9 Oxygenation profiles of MEF cells monitored with cell-penetrating probe MitoXpress®-Intra. After the initial monitoring of resting cells, uncoupler (FCCP at 1 μM) or mock (0 μM) were added at 25 min, followed by the addition of inhibitor AntA at 40 min. Oxygenation conditions are presented in phosphorescence lifetime scale, the range of lifetime and O_2 values is indicated with red lines.

This journal is © The Royal Society of Chemistry 2013

Published on 18 June 2013. Downloaded by University College Cork on 18/06/2013 10:57:28.

differential and asynchronous responses, development and differentiation of stem cells, and transformation of cancerous and diseased cells. It can also be used with 3D cell models, artificial tissue, organs and *in vivo* (see Sections 4.7 and 4.8). Modern imaging systems supporting ratiometric intensity, microsecond FLIM and/or two-photon excitation modes and capable of providing a quantitative readout of O_2 concentration in 2D, 3D and 4D are now widely available.[51,70,75,80]

Using the intracellular O_2 sensing technique with neuronal cancer PC12 cells experiencing local hypoxia, activation of the HIF pathway by intrinsic respiration under ambient pO_2 (19–21%) was demonstrated.[171] In another study, a transient activation of OxPhos in PC12 cells upon depletion of extracellular Ca^{2+} was revealed (not detectable by traditional OCR measurements), and by applying different pharmacological treatments and probes the detailed mechanism of this response was elaborated.[185] Similarly, analysis of the mode of action of the common V-ATPase inhibitor, Bafilomycin A1, revealed its previously unknown uncoupling effect on OxPhos and flickering depolarization of the mitochondria.[112] Mild pharmacological uncoupling with bafilomycin was seen to stabilise HIF-α protein(s) under physiological conditions and induce adaptive responses in colon cancer cell lines.[186] Long-term exposure of neuronal cells to hypoxia (3% O_2 for 30 days) revealed different levels of intra and extracellular O_2 in PC12 and SH-SY5Y cell lines: after adaptation to hypoxic conditions PC12 cells with lower O_2 showed reduced HIF-α signalling.[117] In the latter study, headspace O_2 was monitored using a solid-state OpTech™ sensor (Mocon), along with cellular O_2 analysis.

Due to active consumption of O_2 in the mitochondria and its supply by passive diffusion inside the cell, 'intracellular' O_2 gradients may develop and play physiological roles. Probed using different cell models and techniques, the existence of such gradients under physiological conditions is still controversial and hotly debated.[187–189] Several groups attempted to measure or calculate such gradients, and reported them to be extremely small, below the resolution of current experimental techniques. Thus, in static 2D culture of endothelial cells and the O_2 probe delivered by endocytosis, intracellular O_2 levels were equal to extracellular levels, *i.e.* no gradient.[59] Using the mitochondria-targeted GFP sensor construct, O_2 gradients were also undetectable in Hep3B cells.[190] In contrast, other studies reported the existence of dynamic gradients and anoxic cores in cardiomyocytes.[188,189] Intracellular O_2 probes were used to measure O_2 gradients in lung fibroblasts and neuroblastoma cells which were found to be 1–3 mmHg.[37] In 2D culture of mouse fibroblast cells with active respiration, the gradient between the plasma membrane and intracellular space measured on a TR-F reader was reported to be ~3 μM (at 9% pO_2 or 90 μM).[174] Although these values are close to the measurement error, it can be hypothesized that in cells with active OxPhos, large size and shape resembling their native 3D environments, O_2 gradients under physiological conditions can be significant, while in small cells with low basal respiration (*e.g.* endothelial cells[59]) they hardly exist.

The above examples demonstrate the utility and application potential of O_2 sensing techniques based on cell-penetrating probes. Still better probes are actively sought which can provide more selective, controlled distribution in the cells (cell surface, mitochondria, cytosolic compartments), low toxicity, high brightness, operational and storage stability and convenient use. Active work is on-going, particularly with porphyrin dyes[191] and nanoparticle structures, and new studies are published more and more frequently clarifying important biological questions.

4.7. Tissue models: spheroids, cell aggregates and tissue explants

Cell models which mimic the conditions in 3D tissue include multi-cellular spheroids, cells grown in 3D scaffolds, tissue slices, organ explants and artificial tissue.[128] Multicellular spheroids and cell aggregates[107] are common models in drug screening, toxicity assessment and developmental biology,[128,172] showing *in vivo*-like 3D micro-environment, cell to cell communications, diffusion limited supply of nutrients, pH, CO_2, and particularly O_2. Mapping of O_2 in such models is important, and phosphorescence O_2 sensing techniques are well-suited for that.

Cell-penetrating probes are particularly useful, they can be loaded in spheroid structures and/or cells composing them, and retained for prolonged time. Quenched-phosphorescence O_2 sensing enabled us to demonstrate limited O_2 availability and formation of necrotic core in cancer cell spheroids. Oxygenation of spheroids from primary rat neurons stained with the MitoImage™ probe was visualised by ratiometric intensity imaging under two-photon excitation.[192]

In-depth analysis of objects with sizes >100 μm faces many challenges, particularly for loading with probes and imaging using optical techniques. Using different types of cell-penetrating probes, such conditions were optimised for spheroid cultures of neuronal cells (neurospheres). This method has allowed real-time monitoring of oxygenation of the whole spheroid, and multiplexing with a number of cell biomarkers and fluorescent probes (for intracellular pH, Ca^{2+}, membrane potentials, cell surface markers).[193] Representative images are shown in Fig. 10.

The so-called *ex vivo* models, which include excised tissue slices, biopsies and perfused organs, are used in tumour and developmental biology, studies of cell adhesion, migration, epithelial morphogenesis, and drug testing.[128] Such specimens retain natural 3D organisation and cell–cell interactions, but lack normal O_2 supply by vasculature. They are normally maintained in a 'carbogen' atmosphere (95% O_2, 5% CO_2) to avoid anoxia and cell death. To preserve optimal functional characteristics and viability of such samples, more reliable and accurate control of O_2 and its dynamics is necessary.

Skeletal muscle fibres isolated from frog and microinjected with the Oxyphor™ probe were studied on a custom-built wide-field camera based phosphorescent microscope working in a frequency domain.[61] Dynamics of intracellular O_2 during muscle contraction[194] and at different contraction frequencies,[195] the relationship between aerobic metabolism and fatigue,[196] temperature dependence of intracellular pO_2[197] in muscle fibres were also investigated by this method. Penetration of the PdTCPP probe into the interstitial space of rat spinotrapezius muscles upon topical application allowed the study of average O_2 consumption[198] and

Published on 18 June 2013. Downloaded by University College Cork on 18/06/2013 10:57:28.

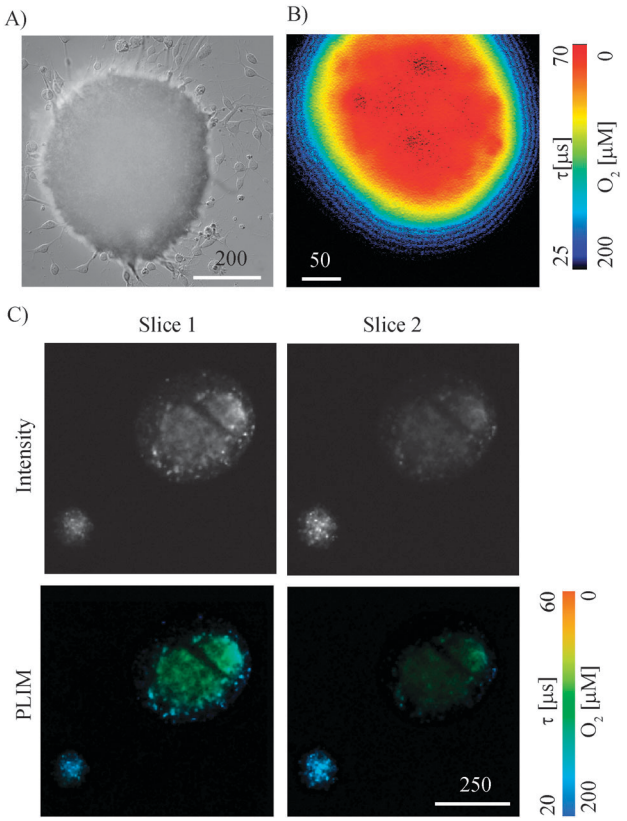

Fig. 10 Phosphorescence intensity (loading) and lifetime (O_2 concentration) images for neurospheres produced by microsecond FLIM microscopy and cell-penetrating O_2 probes. (A) Differential interference contrast image of a proliferating neurosphere; (B) widefield FLIM image of a neurosphere stained with MitoImage™ NanO2 probe; (C) optical sections (10 μm each) of confocal FLIM-TCSPC and intensity images of neurosphere stained with PtPFPP conjugate. The false-colour FLIM images provide information on the O_2 levels across the spheroid. Scale bar is in μm.

dependence of oxygen availability in skeletal muscle,[199] revealing a sigmoid dependence of VO_2 on pO_2.[200]

Carotid body is a specialised organ which senses changes in arterial oxygen and regulates respiration and lungs function. *Ex vivo* analysis of type I oxygen sensing cells was conducted by dynamic multifocal microscopy imaging of intracellular O_2 (with PEPP0[201] probe), together with Ca^{2+} and membrane potential, revealing the heterogeneous responses of different cells in the carotid body.[202]

Respiration and physiology of salivary glands isolated from an insect (blowfly *Calliphora vicina*) were studied by injecting the PtPFPP-based 300 nm polystyrene microparticles and lifetime-based detection of O_2 by phase fluorometry on a custom-made microscope.[203,204] Using this set-up, authors also performed quantitative imaging of intracellular pH and extracellular O_2 in this tissue under resting and stimulated conditions and demonstrated the regulation of intracellular pH by V-ATPase and carbonic anhydrase.[204]

Cell-impermeable O_2 sensors were also applied for mapping O_2 in 3D cell cultures, including the PDMS microparticles (5–40 μm) with Ru-dye and intensity imaging of hydrogel scaffolds,[205] silica beads with Ru-dye to image oxygenation of chondrogenic cells in aggregates and spheroids.[206] More recently, ratiometric Ru-dye based nanosensors with Nile Blue[207] or coumarin 540[69] reference dyes were produced and used for O_2 imaging in 3D culture of colon intestinal cancer cells and the microfluidic tumor model by fluorescence microscopy. Fibre-optic O_2 sensors were applied to measure O_2 in porcine muscle in a tissue perfusion system.[208] OCR and viability measurements in whole porcine kidneys allowed differentiation of healthy and damaged organs, thus providing a useful quality control tool for organ transplantation.[209] Unfortunately, in some of these studies, qualitative rather than quantitative O_2 analysis was conducted, which reduces their value.

New materials for tissue engineering and organ transplantation must be analysed for their biocompatibility and functional properties. A Ru-based solid-state O_2 sensor was applied to study O_2 diffusion across pulmonary surfactant layers to reveal that O_2 diffusion in surfactant layers is significantly higher than in the water phase.[210]

4.8. *In vivo* and *ex vivo* measurements

O_2 levels in different tissues and cells of our body normally range 0.5–10%.[8,211] They are highest in the lungs from which O_2 is supplied to other tissues by the blood through a network of vessels and micro-capillaries. O_2 demand is determined by the metabolic state and respiratory activity of tissue (mainly OxPhos and mitochondrial function), while supply – by blood flow, oxygenation (influenced by many biochemical parameters), O_2 diffusion and steady-state O_2 gradients within tissue. O_2 distribution and dynamics are specific for each tissue and critical for their physiological functions.[188,212–219] Normal homeostatic conditions *in vivo* are called *physiological* normoxia. Hypoxia and anoxia denote substantially reduced and zero levels of O_2. These abnormal conditions lead to pathological states, development of disease and ultimately death.

Quenched phosphorescence methods have long been applied to *in vivo* measurements of O_2.[6,217,220] We mainly focus on the new applications with *quantitative* O_2 measurements and corresponding methodologies revealing novel biological results. The non-biological and qualitative studies, as well as alternative hypoxia-specific probes (Table 1), are omitted.

High intrinsic absorption and scattering of animal tissue demand probes with longwave or multi-photon excitation and emission in the range 600–900 nm, with high brightness and photostability for high-resolution 3D imaging. Extracellular, cell-impermeable probes injected intravenously in live animals are most commonly used. These probes are required to be inert, have good biocompatibility and distribution in the tissue of interest, long clearance times, low accumulation in organs and systemic toxicity. Recent modelling demonstrated that for microscopic and high resolution measurements, the phosphors do not have to be confined in the region of interest and can be distributed throughout the volume.[221]

Probes based on PdTCPP and Pd-TBP dendrimers (Oxyphor™ family[18] from Oxygen Enterprises) are most commonly used. They have moderate solubility and inertness, optimal spectral

 This journal is © The Royal Society of Chemistry 2013

Published on 18 June 2013. Downloaded by University College Cork on 18/06/2013 10:57:28.

characteristics and sensitivity to O_2, distribution and retention in the body, and are seemingly non-toxic. Initially they were used in low-resolution point and 2D measurements under one-photon excitation. The new structures, such as PtP-C343 probe with light-harvesting antennae and PEGylated shell, have enabled high-resolution, 3D and multiphoton O_2 imaging with excellent analytical performance[75] (though they are difficult to synthesise, expensive to use and require specialised set-up – two-photon microsecond FLIM).

These intravital O_2 probes were applied to study cerebral vasculature, neuronal activity,[73,222–225] tumor oxygenation,[226] microcirculation,[217] muscle physiology,[194,197,227] for mapping O_2 tension in retina[228] and tomographic imaging at the macroscopic level.[229] Topical application of the PdTCPP probe and one-photon time-gated phosphorescence quenching microscopy[62,228,230,231] were used in *ex vivo* studies of pO_2 near arterioles and oxygen consumption in rat mesentery,[230] where no difference in pO_2 profiles between small and large arterioles and similar pO_2 values between interstitial and intravascular compartments were observed. O_2 loss from mesenteric arterioles was also shown to be moderate and close to theoretical predictions and results produced by other groups.[232] These applications are reviewed in more detail in ref. 217.

Point measurements of O_2 were also used. Thus, *in vivo* function of AMP-activated kinase, a master regulator of cell bioenergetics, is poorly understood. It was examined using the Oxyphor R2 probe and frequency-domain phosphorometry. Analysis of microvascular dynamics of pO_2 during contractions of mouse muscles demonstrated that O_2 delivery is affected by AMPK activation.[227] Similarly, myocardial function was studied directly in the beating heart using the Oxyphor G3 probe injected in three myocardial areas.[200] Several set-ups were proposed for pO_2 mapping in retina,[228,233–236] and optimisation measurements to avoid vascular damage and degeneration of the optic nerve.[237] Modulation of vascular pO_2 in retina by light was demonstrated,[235] and used in the concept of wireless intraocular microrobots.[238]

Hypoxia is one of the hallmarks of cancer,[239] it contributes to tumour aggressiveness and metastatic potential, and efficiency of anti-cancer therapy. Tumour oxygenation was long thought to be regulated by diffusion, however, phosphorescent imaging with the Oxyphor G2 probe has revealed that various tumours (fibrosarcomas, carcinomas and gliomas) display dynamic patterns of oxygenation with spatial and temporal heterogeneity.[226] New Oxyphor R4 and G4 probes, which can operate under protein-rich conditions such as blood plasma and interstitial space and have relatively long retention times (hours),[64] also demonstrated increased accumulation in tumours. This can be explained by the higher permeability and the retention effect of tumour tissue.[240] Tumor targeting of O_2 probes (*e.g.* with antibodies or other 'vectors') can also facilitate imaging of tumours.[241] Imaging of mouse tumours with Oxyphor G4 on a widefield macroscope showed that anaesthesia with isoflurane affects tissue oxygenation.[74]

The most advanced probe of this type, PtP–C343 (τ_0 = 60 μs, k_Q = 150 $mmHg^{-1}$ s^{-1}),[59,60] was used to measure oxygenation of vasculature in live animal brain by two-photon microsecond FLIM and analyse function of regions of the brain in 3D.[59,242] Simultaneous imaging of blood flow and oxygenation in rat cerebellum with penetration depth of up to 300 μm and spatial resolution of ~1 μm was demonstrated,[224] and used to create a biophysical model of multicompartments in cerebral vasculature.[223,243] Analysis of vasculature and tissue oxygenation in rat somatosensory cortex under resting and stimulated conditions showed that stimulus-evoked increase of tissue pO_2 is dependent on the baseline O_2 levels.[220] pO_2 in brain vasculature and Ca^{2+} dynamics during neuronal activation by inhalation of an odorant,[224] and monitoring of pO_2 transients in capillaries and local neuronal activity in rodent brain were studied.[225] Amazingly, two-photon microscopy also revealed local O_2 gradients around individual erythrocytes in blood microvessels.[225]

Planar sensors (PtOEP dye in polystyrene on a polyester support) were used to image O_2 in the dorsal skinfold chamber model with amelanotic melanoma,[244] confirming lower mean O_2 values in tumour regions than in normal skin. The sensor data were compared with the electrode method[245] which produced higher O_2 values for capillary blood samples, and this was explained by O_2 consumption by the electrode. Similarly, ischemia-reperfusion experiments with sensor film on forearm demonstrated the anticipated fluctuations of O_2 in microcirculation.[245] Sensor foil was also proposed for the study of skin cancer development, wound healing,[214,246] and the role of stratum corneum in epidermal oxygen barrier.[246]

Planar sensor foil was applied to monitor oxygenation of rat brain cortex[247,248] (qualitatively, using a light-conducting PMMA cylinder, ring of 405 nm LEDs and a small CCD camera assembled on animal head), detection of radial O_2 gradients across cortex arterioles.[247,248] Another ratiometric planar film sensor was applied to monitor brain activity and also proposed for use in conjunction with electrophysiology to monitor other analytes in interstitial space during spontaneous seizure-like events.[249] Similarly, progression of trauma patients towards hemorrhagic shock was monitored *via* oxygenation of the peripheral tissue of model animals (piglets) using a needle-type microsensor containing a solution Oxyphor G3 at its tip.[250]

A new cell-penetrating probe, NanO2-IR, was applied topically to quickly stain rat brain neocortex, and then monitor through a cranial window responses to peripheral sensory stimulation (whisker model) in the live animal. Dynamics of oxygenation in selected regions of brain tissue was monitored on a standard animal imager in 2D, and correlated with the data produced by a fluorescent potentiometric probe revealing considerable differences.[251]

A few other phosphors were proposed for *in vivo* O_2 imaging. $Ir(btp)_2(acac)$ bound to albumin was applied for semi-quantitative intensity-based O_2 imaging in rodent tumour tissue.[182,252] This probe showed broad distribution in tissues and efficient internalisation, it was later modified with coumarin C343 to enable ratiometric imaging[253] (though its photostability may be an issue). Similarly, Ru-complexes were proposed for imaging of tissue hypoxia.[254]

O_2 sensing by quenching of delayed fluorescence of endogenous protoporphyrin IX (PPIX) was described. The procedure

Published on 18 June 2013. Downloaded by University College Cork on 18/06/2013 10:57:28.

involves administration of 5-aminolevulinic acid – a precursor in PPIX biosynthesis, which increases the levels of mitochondrial PPIX (this approach is used in photodynamic tumour therapy, PDT[255]), and detection of red emission of PPIX sensitive to O_2.[37,256–260] Known localisation of PPIX enables to probe mitochondrial/intracellular O_2.[37] The drawbacks of this method are poor photostability and brightness of PPIX, phototoxicity and physiological consequences of PPIX overload.[261] Point measurements with an optical fibre (1000 μm) and 510 nm excitation have limited spatial resolution and in-depth penetration, giving average pO_2 values, but they are well-suited for O_2 measurements on the skin surface. Measurements of rat skin produced O_2 values were comparable to those for skeletal muscle.[258] Analysis of perfused heart demonstrated that mitochondrial O_2 levels *in vivo* are higher and more heterogeneous than were previously thought.[259] O_2 monitoring in perfused liver[260] and in tumor tissue undergoing PDT[262] (which depends on the available O_2[261]) were also reported. As a model of vascular damage in PDT, the chorioallantoic membrane of chicken egg demonstrated good correlation between the damage during PDT and tissue hypoxia.[262]

In the future, increased use of such materials and sensing techniques, and development of new probes with improved biocompatibility, brightness and targeting properties, suitable for high-resolution, quantitative O_2 imaging and compatible with standard detection platforms such as multiphoton microscopes and animal imagers are envisaged.

4.9. O_2 in plants

Plants produce O_2 by photosynthesis and consume by respiration, these light-dependent and 'dark' metabolic pathways are coupled and cross-regulated. Evolved from aquatic photosynthetic organisms, plants also have specialised mechanisms to regulate metabolism and cope with low O_2 availability (hypoxia is a common condition in plant tissues, seeds and roots during soil flooding[9]). Understanding of this regulation is important for basic plant science and agriculture.

Plants possess a rigid carbohydrate cell wall which makes it rather difficult to interrogate plant tissue and conduct O_2 measurements. This natural barrier can be overcome by using needle-type microsensors, microinjection, or delivery of soluble O_2 probes through the root and circulating fluids. Strong autofluorescence (chlorophyll in leaves, carotene and other pigments) can interfere with sensor signals, particularly in intensity and phase measurements. The rooted zone of plants, called the rhizosphere, is a dynamic system which includes symbiotic bacteria, nematodes and other organisms, regulates nutrient storage, nitrogen fixation, biosynthesis pathways of the plant, and the global cycle of biogenic elements and chemicals.

Similar to animal cells and tissues, phosphorescent sensors are useful for bioenergetic studies of plant compartments.[263] Potato tubers with active metabolism and diffusion-limited supply of O_2 creating hypoxic conditions are popular models. During their lifespan tubers experience different environmental conditions, from deep hypoxia in flooded soil to 21% O_2 during storage. Regulation of sugar metabolism by O_2 during tuber development was measured with an O_2 micro-sensor to elaborate the roles of pyruvate and alternative oxidase.[264] Similar to animal cells, plants contain hypoxia-responsive elements, particularly the ethylene-response factor (ERF) which regulates a spectrum of genes during tuber development.[9] O_2-dependent expression of these genes in different compartments was investigated using O_2 microsensors.[265,266] A micromanipulator allowed microinjections in cells and in-depth measurement. Similarly, hypoxic regulation of metabolism in the roots of pea and *Arabidopsis* and dynamics of O_2 gradients in the root zone upon stimulation with pyruvate were analysed.[267]

A simple imaging system, VisiSens (PreSens) operating with planar sensor foil, was used to study oxygenation of plant surface and underlying vasculature.[268,269] Providing 20 μm spatial resolution, it was applied to seed, leaf, stem sections and the rhizosphere *of Cabomba caroliniana* (water plant), *Tradescantia fluminensis* (ground plant).[268] Photosynthetic O_2 production and consumption by respiration under alternating light and dark conditions, upon inhibition of photosynthesis by 3-(3,4-dichlorophenyl)-1,1-dimethylurea,[269] and in plants infected by bacteria were also studied.

Exchange of gases, particularly O_2, plays important roles in ripening of fruits and their behaviour under ambient and preservation conditions. Optical O_2 sensing was used to monitor soft fruits and vegetables and their surroundings. Hypoxia in tomato fruits was probed with a fiber-optic microsensor.[270]

Analysis of the quality and germination potential of plant and vegetable seeds is another important application.[271] This can be performed in dedicated micro-well plates with O_2 sensors. One seed with a small amount of water is placed in each well, and then a uniform gas-tight sealing of the wells is applied followed by the monitoring of seed respiration (several hours per day). The gas–liquid system is optimised to activate metabolism and germination of the seed, but not to 'flood' or suffocate it. Rational assay design (plate material, seal, volume ratio of the well/added liquid/seed, respiration activity) enabled us to achieve reproducible results. Fig. 11 shows typical respiration profiles, with a robust change of metabolism from anaerobic to aerobic for the viable but not dead seeds, and their different germination potential. After the non-invasive testing, healthy seeds can be extracted by puncturing the seal and planted. This helps to avoid planting of non-viable material, optimise storage conditions and treatments, test efficiency of herbicides and other factors on the quality of elite seed material. Commercial systems are being developed by Astec Global and other companies.

A solid-state PtPFPP based sensor coupled with neutron radiography was applied to monitor O_2 and H_2O in root zone during night and day phases,[272] providing a powerful platform for plant biochemistry and metabolism.

4.10. Control of O_2 in fluidic systems, cell based biochips and bioreactors

Perfusion chambers, microfluidic devices and biochips allow rapid, miniaturised and parallel analyses of test cells and tissue, with exposure to various conditions. These systems

 This journal is © The Royal Society of Chemistry 2013

Published on 18 June 2013. Downloaded by University College Cork on 18/06/2013 10:57:28.

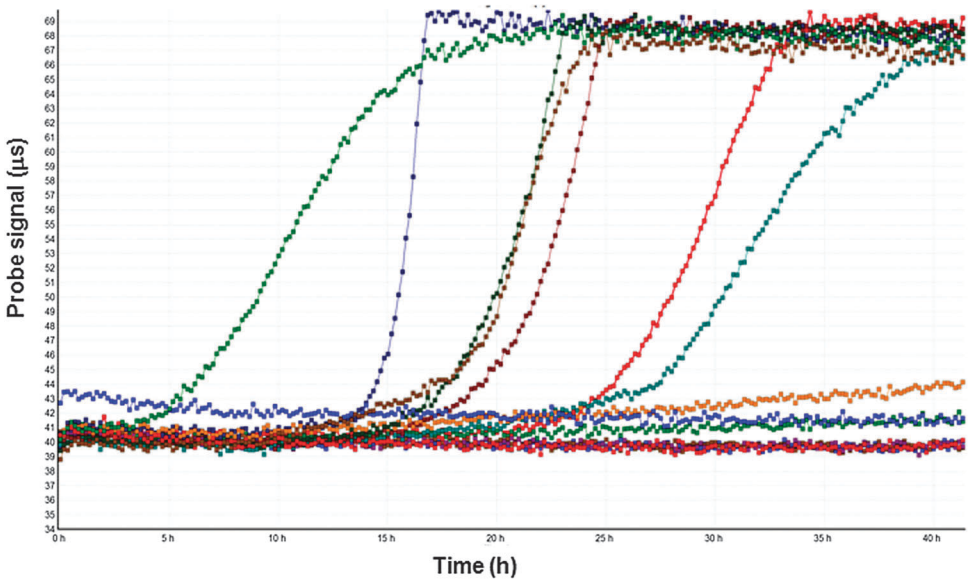

Fig. 11 Assessment of viability of individual seeds by O_2 micro-respirometry (courtesy of Luxcel Biosciences).

can provide large amounts of data, save valuable biomaterials, time and costs,[173] but are also facing many challenges. To produce plausible biological data and interpret the results correctly, reliable control of oxygenation conditions is required for such systems, to avoid cell stress by transient or sustained hypoxia, anoxia or hyperoxia. Even in macroscopic cultures, respiring samples face O_2 limitation (see Section 4.6), altered cell function or death.[172] Stable supply of O_2 can be achieved by dynamic flow conditions,[146,173] but small dimensions of such devices, the need for servicing and priming (particularly seeding the cells and letting them to adhere to the surface), require stopped flow conditions which may lead to fast anoxia.[173] This can be overcome by using biochip materials highly permeable to O_2 such as PDMS.[273] Biochips integrated with O_2 probes or solid-state sensors[173,273–275] and tailored to O_2 sensing and imaging experiments[82,146,173] were also described. Control of cell oxygenation combined with 'metabolomics-on-a-chip' analysis using ^{1}H-NMR provides a powerful tool for studies of tissue function.[276]

New ways to manipulate using O_2 concentration and regulate cellular function can also be implemented. Thus, O_2 gradients can be produced by mixing gases inside the PDMS chips controlled with an O_2 sensor,[277,278] or by chemical consumption O_2 in channels separated by a gas-diffusion membrane.[147,279] The effect of O_2 availability on the action of an anti-cancer drug on cells was studied.[279] A microfluidic device with polycarbonate coating (to minimise back diffusion of O_2 through PDMS) was applied to study hypoxia-dependent migration of breast cancer cells in 3D collagen scaffolds,[280] showing that ~3.9% hypoxia (compared to 8.5% O_2 in normal breast tissue) promoted directional motility of cancer cells. Biochips with O_2 sensors allowed modelling of O_2 gradients and shear stress, and design of novel bioreactors and 3D scaffolds.[275,281] Fluidic inserts with Ru-based sensors were used to modulate O_2 levels and study heterogeneity of adherent cells in standard microtitre plates.[282]

Many existing microfluidic devices can be adapted for O_2 sensing with soluble O_2 probes. Small-size microchannel based devices such as µ-slides (Ibidi) provide high sensitivity in OCR measurements under static conditions, cell perfusion and multiple treatments, and multiplexed detection of other biomarkers (fluorescent probes, immunostaining) to study drug effects on cell bioenergetics.[283]

O_2 sensors have been used in macro-scale bioreactors to monitor dissolved and headspace O_2 during fermentations with microbial cells.[284] High rates of O_2 utilisation make O_2 availability one of the main limiting factors, and feedback control through optimal aeration and stirring provides faster and higher yield of target products and reduces energy and costs. Conversely, stress of the cells due to O_2 limitation results in reduced biomass and/or expression of target products (proteins or metabolites).

In array-type micro-bioreactors O_2 monitoring is also necessary. Customised sensor systems, coated microplates and SensorDish reader (PreSens)[285] were applied to study cultivation conditions and media with yeast,[286,287] bacterial, mammalian and plant cell cultures.[288,289,290]

Design of new biofermentation systems and micro-bioreactors provides good scope for soluble O_2 probes, *e.g.* monitoring of yeast fermentation with ratiometric nanoparticle sensors.[291] Magnetic microparticle sensors manipulated inside the fermenter were also demonstrated with bacterial cultures.[65]

Generally, macroscopic solid-state sensors with an integrated optoelectronic module or optical fibre connection mounted on the reactor vessel can be used in fermentations performed on a large scale, with bioproducts intended for human consumption (for which even minute contamination with sensor material is highly undesirable – regulated by FDA). Soluble O_2 probes are better suited for laboratory systems, process optimisation and pilot studies performed on a small scale in a combinatorial and high throughput format.

Published on 18 June 2013. Downloaded by University College Cork on 18/06/2013 10:57:28.

4.11. Respiration of whole organisms, biochemical and environmental toxicology

Total respiration of an organism is a useful biochemical indicator of its development, metabolism, adaptation to changing conditions.[292] Toxicological assessment of chemical, biological and environmental samples using such models is a growing research area. Small aquatic organisms such as *Daphnia magna*, *Artemia salina* and *Danio rerio* (zebrafish), as well as soil worms *C. elegans*[142] are convenient models for acute toxicity testing. They have been applied to analyse heavy metal ions, pesticides, environmental samples such as fresh, sea and wastewater, soil by optical micro-respirometry, showing superiority to traditional toxicity assays based on mortality or morbidity assessment of model organisms.[293,294] OCR is a generic and sensitive marker of toxicity detecting sub-lethal effects *via* both inhibition or activation respiration. The format described for cells (standard microplate, MitoXpress®-Xtra probe, TR-F reader detection) is also applicable to these organisms, allowing the generation of dose–response curves and patterns of toxicity (on a panel of different organisms) and processing of large number of samples in an automated fashion. This is an attractive alternative to toxicity testing using higher animals (fish, mammals).

Fatty acid metabolism is important in the adaptation of fishes to water composition and is related to mitochondrial function. It was analysed in developing dover sole fish (*Solea solea*) under hypoxia with a solid-state O_2 sensor,[295] revealing that depending on the diet, larvae have different metabolic rates, tolerance to hypoxia and metamorphosis rate. Spatio-temporal dynamics of O_2 at the surface of corals was probed with specially designed magnetic sensor microparticles.[296] Cyanobacteria *Synechocystis* sp. PCC6803 monitored using a planar O_2 sensor showed a higher photosynthetic activity in the exponential phase than in the stationary phase,[297] which can be explored in biofuel production by direct photoconversion. Biodegradation of many hydrocarbons (*e.g.* chlorobenzene by 1,2-dioxygenase enzymes) is highly dependent on O_2. Using O_2 sensors, microaerophilic organisms living at reduced O_2 levels (<60 μM O_2) were shown to have potential for industrial biodegradation processes.[298] A fiber-optic O_2 minisensor was applied in long-term (450 h) batch-monitoring of dissolved organic carbon biodegradation.[299]

Environmental O_2 affects behaviour and migration of many soil residents such as *C. elegans* nematodes.[300] The NanO2 probe and wide-field microsecond FLIM microscopy were used to study O_2-dependent behaviour of the worms fed with *E. coli* on agar plates. Under ambient air conditions the worms were seen to gather in clumps where they create low O_2 (0–5%) conditions.[70]

4.12. Trace and low oxygen analysis in marine, aquatic, soil and environmental biology

Since the emergence of life on the planet until present days, O_2 levels in the atmosphere, ocean and the lithosphere have been closely connected. Starting from very low levels ($<0.01\%$ v/v),[301] O_2 pollution by evolved photosynthetic cyanobacteria and plants, has brought us to current levels of 20.86% O_2 in the atmosphere. This transition was accompanied by a major change in living systems from anaerobic to aerobic metabolism.[302] Anaerobic and deeply hypoxic environments still exist in many parts (deep biosphere) and are populated with primitive organisms. They often host large communities of different species (anaerobes, microaerophiles and others[1,2]). Functional organisation and metabolism in these niches with living matter are poorly understood, hard to access or reproduce under laboratory conditions, and their roles in the emergence of carbon-based life and higher organisms (studied much better) remain elusive.

The challenges here are the precise control of very low O_2 levels and respiration rates.[130,302] Polarographic (electrode-based) and many other methods become unusable for this. Standard O_2 sensors can work reliably at 0.05% O_2, the phosphorescent method can be easily adapted for much lower ranges. There are many phosphors with long emission lifetimes (>500 μs) and polymeric matrices providing high K_{S-V}. Thus, the Fibox 3 trace system (PreSens) based on the PtPFPP dye in a fluorinated polymer,[303] PtTPTBPF based microsensors[304] and polymeric films of fullerene C_{70}[305,306] were suggested for trace O_2 analysis.

The cryosphere, which includes glaciers, ice sheets, and Antarctic sub-glacial lakes, is an extreme environment which also hosts communities of microorganisms, with O_2 concentration determined by the balance between photosynthesis, respiration and chemosynthetic processes such as sulphide oxidation. Detection of O_2 in the cryosphere using optical sensors has been demonstrated,[306] and optimisation of sensor design resulted in fast response times, high sensitivity, minimal temperature dependence and signal drift.[303]

Open ocean covers 92% of the sea floor and has an average depth of >200 m. Photosynthesis in such an environment is determined by light penetration, available nutrients and substrates, and is limited to the 'photic zone' of ~100 m. In deep ocean suboxic (<4.5 μM O_2 and <1 μM H_2S) and anoxic zones are common, but they are stratified.[307] Such zones occupy only ~1% of global ocean, but contribute to about 1/3 of the loss of nitrogen in the ocean *via* denitrification.[308] For deep sea benthic layers, specialised sensor systems have been developed which measure O_2 consumption in multiple sites on the sea floor.[309–311] These sensor systems are usually optimised for long-term measurements, autonomous or cabled and coupled with other measurement devices (*e.g.* photocamera, acoustic, sedimentation sensors). Analysis of sub-mm niches with reducing conditions in benthic fauna require high resolution imaging of O_2 (also CO_2 and pH).[312] It was hypothesized that in heterogeneous sediments such micro-niches play significant roles in the accumulation of trace metals, scavenging and fossilisation. Here needle-type and planar O_2 sensors demonstrated high stability, quick response times, non-invasiveness and imaging capabilities.[312] Film sensors were also used to probe underground water capillary fringes.[313]

In marine biology, macro-methods allow monitoring of net biological production, air–sea O_2 exchange, salinity, geological processes. Seasonal factors and O_2 availability regulate the life of aquatic communities of protozoa and higher organisms,

 This journal is © The Royal Society of Chemistry 2013

Published on 18 June 2013. Downloaded by University College Cork on 18/06/2013 10:57:28.

which requires investigation.[2] Traditional electrode-based systems[314] are now complemented by optical O_2 sensors. Fibre-optic O_2 and CO_2 sensors (*e.g.* Aanderaa, Ocean Optics, PreSens), allow the analysis of marine environments, discrete colonies and individual (micro)organisms on a micro-scale. A dedicated autonomous FerryBox system[315,316] allows monitoring for >1 year, is insensitive to temperature and salinity, flexible and affordable.[307,317] A dual O_2–CO_2 sensor for aquatic systems is also described.[318] In freshwater systems steep O_2 gradients and stratification effects can also be prominent. Respiration of freshwater communities of bacteria and plankton in a cuvette format were also measured, with sensitivity at about 2.2 million cells per ml.[319] Analysis of trace O_2 and microaerobic organisms is expected to develop rapidly.

4.13. Data processing and measurement artefacts

With increasing use of the O_2 sensing techniques, processing of experimental data is becoming important, especially for measurements with complex and gentle biological samples and in applications requiring high accuracy and reliability of O_2 quantification or dealing with large amount of experimental data (screening or imaging).

A dedicated data processing algorithm was developed for screening OCR assays in microplates, in which raw profiles of phosphorescence lifetime or intensity signals are transformed into the double-reciprocal plots and then processed using the pairwise reading method. This approach provides more accurate and statistically plausible OCR values, it was initially demonstrated with simple enzymatic reactions and then applied to screening of compound libraries with isolated mitochondria.[320] It also works well with sealed cuvettes and capillary platforms.[93]

O_2 imaging, especially FLIM, 3D and time-lapse experiments also require special algorithms to cope with massive volume of data, and process them on-line. Some vendors of laboratory equipment are starting to offer dedicated templates, scripts and software for selected applications based on quenched-phosphorescence O_2 sensing. Examples include fluorescence readers from BMG, FLIM microscopes from Becker&Hickl and LaVision, O_2 probes from Luxcel, GreenLight® systems from Mocon.

Measurement artefacts are also quite common in this area. They are usually associated with incorrect quantification of O_2 misinterpretation of O_2 sensing data, and, the worst case, of the biological results produced. Some common sources of errors are:

(1) Effects of temperature equilibration of the sample or absence of reliable *T*-control during measurements particularly at elevated temperatures (37 °C). For example, in microplate assays with multiple samples, plate equilibration is evident over the first 5–20 min. Some instruments produce non-uniform *T*-maps and pronounced plate effects. This must be considered by optimisation, physical modelling of sample and sensor behaviour, or disregarding the initial part from quantitative analysis.

(2) Unstable or inaccurate O_2 calibration of the system, which includes the sensor, sample and instrument, for given experimental conditions. Calibration can be performed inadequately or affected by sample optical properties, interfering substances, pH, ionic strength. Sensors with high temperature coefficients, complex shape of calibration (non-linear Stern–Volmer dependence[67]) or limited stability should be avoided and replaced with more stable and robust materials.

(3) Low probe concentrations or loading efficiency, non-uniform loading of the sample or probe localisation in specific compartments (*e.g.* vasculature, interstitial space, but not inside cells). Photounstable probes can bleach rapidly. Low and unstable optical signals and high binning may result in significant measurement noise, skewed calibration, or parts of the sample being unavailable for O_2 analysis.

(4) Cyto- and photo-toxicity of the probe due to its non-biogenic nature, photophysical characteristics distribution within the cell (*e.g.* in membranes, mitochondria, nuclei) or high doses used. Shortwave excitation (*e.g.* with 365, 405 and even 488 nm lasers) also causes direct photodamage of cells. Optimisation of the probe, loading method, and use of red and two-photon excitable (600–900 nm) phosphors[18,75] or up-converting nanoparticles[321] help to minimise this.

(5) Incorrect measurement settings on the instrument or blind conversion of sensor signals into O_2 concentration (common for many commercial systems) may produce unusual respiration profiles, OCR values and biological results.[101] Excessive excitation can cause photosensitization and photodamage of the sample and sensor material through generation of high levels of singlet oxygen and ROS. Thus, phosphorescent imaging with large excitation area and high repetition rate of excitation pulses leads to significant photoconsumption of O_2 resulting in measurement artefacts.[217] This can be overcome using the Small Excitation Area method.[322]

(6) Perturbed mass exchange and O_2 diffusion in the sample can strongly influence the accuracy of measurements. Uncontrolled leak of ambient O_2 through vessel material (plastic), broken seal, contact with gaseous phase, additional barrier introduced by the measurement system,[323] or photoconsumption of O_2 can strongly influence the results. Back-diffusion of ambient O_2 can be reduced by barrier materials (*e.g.* glass-coated plates), special assay vessels,[105] or compensated by physical modelling.[106,171]

Another group of artefacts is more specific to particular O_2 sensing formats and bioassays. For example, when changes in O_2 concentration occur very fast (*e.g.* in samples with high microbial load, OCR or enzyme activity), intensity based sensing may deliver a false-negative result as both fully aerated and deoxygenated conditions produce constant signal. Lifetime-based sensing overcomes this as it unambiguously informs on O_2 levels.

Planar sensor foil with O_2-impermeable support also has drawbacks. For optical measurements the specimens are usually adhered tightly to the foil (sometimes flattened and sliced), and this may impose mechanical stress, alter natural aeration conditions and produce different results.[244] Artefacts in tissue O_2 measurement caused by mechanical stress were also reported for needle-type sensors and microelectrodes.[6]

Measurement of cellular responses in an open plate with an intracellular O_2 probe also requires conditions where resting cells partly deoxygenate themselves (basal oxygenation). If they

Published on 18 June 2013. Downloaded by University College Cork on 18/06/2013 10:57:28.

appear to be fully oxygenated or deoxygenated, changes in respiration upon stimulation may be undetectable: uncoupling of deoxygenated cells or inhibition of air-saturated cells cannot be seen on the profiles.[184] Cell oxygenation levels and optical responses can be tuned by optimising cell density or performing measurements at reduced pO_2. Mechanical distortion of the plate and effector addition can affect steady-state deoxygenation, gentle dispensing and handing of the plate helps eliminate this.

In summary, when introducing a new probe, method, measurement set-up or application based on quenched-phosphorescence O_2 sensing, they should be carefully examined for presence of such issues and degree of their severity. Analysis of primary signals from the sensor (intensity and lifetime), control samples, blanks and artificial simulations proved very useful for working out adequate measurement, signal acquisition and data processing strategies.

5. Future outlook

The above sections and examples show the high utility and tremendous potential of optical O_2 sensing in the field of biological detection. Many exciting developments, studies with different models and objects and ground breaking biological results have been produced so far. The area is set to develop rapidly for the next 5–10 years.

In basic life sciences and medicine, detailed mechanistic studies of cellular function, physiology of cell, tissue and whole organisms, stem cell technologies, tissue engineering, hypoxia research will be high on the agenda. O_2 sensing technologies are indispensable research tools here, gradually approaching their ultimate targets – diagnostics, therapeutics and human use. On the application side, growing use of biodetection systems based on O_2 sensing is envisaged, particularly in rapidly emerging large-volume applications such as microbial and food safety, security and biodefence, drug screening and toxicity testing, control of agricultural and pharmaceutical products, medical devices and bioprocessing, environmental monitoring.

The following main trends in development of such O_2 sensing systems are seen: (1) broader use of established O_2 sensing platforms, particularly fibre-optic (micro)sensors, phosphorescent readers, live-cell and animal imaging systems, intravital systems, as routine research and laboratory tools; (2) deeper integration of optical O_2 sensing technologies with advanced photonics, nanomaterials, micro and nanofabrication[324] on the one hand, and cell and tissue engineering, stem cell technology, regenerative medicine and *in vivo* experimentation on the other;[128,325] (3) wider use of imaging modalities and digital photography, development of hi-spec and super-resolution platforms, as well as portable low-cost bioimaging solutions (*e.g.* microscope on a chip[49]); (4) development of interactive and intelligent sensor systems providing remote control, wireless communication and autonomous operation; (5) flexible architecture and convergence of optical O_2 sensor technology with other bioanalytical platforms. Further miniaturisation and development of sensor chips, in-field, personal care and implantable devices; (6) design of advanced sensing materials with improved biocompatibility, analytical performance and flexibility produced by rational design for *in vivo* and *ex vivo* use; and (7) development and deployment of specialised bioanalytical platforms, integrated systems and solutions for the life, medical and environmental sciences.

Abbreviations

ADP	Adenosine-diphosphate
AMP	Adenosine-monophosphate
AOAC	Association of official analytical chemists
ATP	Adenosine-triphosphate
CCD	Charge coupled device
CMOS	Complementary metal-oxide semiconductor
ECA	Extracellular acidification
ELISA	Enzyme-linked immunosorbent assay
ERF	Ethylene-response factor
ETC	Electron transport chain
FCCP	Carbonyl cyanide 4-(trifluoromethoxy)phenylhydrazone
FDA	Food and drug administration
FLIM	Fluorescence/phosphorescence lifetime imaging microscopy
GFP	Green fluorescent protein
HIF	Hypoxia inducible factor
LED	Light-emitting diode
MAP	Modified atmosphere packaging
MRSA	Methicillin-resistant *Staphylococcus aureus*
NIR	Near infrared
OATP	Organic anion transporting polypeptide
OCR	Oxygen consumption rate
OxPhos	Oxidative phosphorylation
PDMS	Poly(dimethylsiloxane)
PDT	Photodynamic therapy
PEG	Poly(ethyleneglycol)
PMT	Photomultiplier tube
PPIX	Protoporphyrin IX
RLD	Rapid lifetime determination
ROS	Reactive oxygen species
SAR	Structure–activity relationships
TCSPC	Time-correlated single photon counting
TR-F	Time-resolved fluorescence
TVC	Total aerobic viable counts

Acknowledgements

This work was supported by the Science Foundation Ireland, grants 07/IN./B1804 and 12/TIDA/B2413, the Department of Agriculture, Food and Marine, grant DAFM 11/F/015, and the European Commission FP7 Program, grant FP7-HEALTH-2012-INNOVATION-304842-2.

Notes and references

1 R. L. Morris and T. M. Schmidt, *Nat. Rev. Microbiol.*, 2013, **11**, 205–212.
2 T. Fenchel and B. Finlay, *Biol. Rev.*, 2008, **83**, 553–569.

 This journal is © The Royal Society of Chemistry 2013

Published on 18 June 2013. Downloaded by University College Cork on 18/06/2013 10:57:28.

3 N. Nelson, *Biochim. Biophys. Acta, Bioenerg.*, 2011, **1807**, 856–863.
4 S. Ball, C. Colleoni, U. Cenci, J. N. Raj and C. Tirtiaux, *J. Exp. Bot.*, 2011, **62**, 1775–1801.
5 M. D. Brand and D. G. Nicholls, *Biochem. J.*, 2011, **435**, 297.
6 D. F. Wilson, *Am. J. Physiol.: Heart Circ. Physiol.*, 2008, **294**, H11–H13.
7 G. L. Semenza, *Wiley Interdiscip. Rev.: Syst. Biol. Med.*, 2010, **2**, 336–361.
8 M. Erecinska and I. A. Silver, *Respir. Physiol.*, 2001, **128**, 263–276.
9 J. Bailey-Serres, T. Fukao, D. J. Gibbs, M. J. Holdsworth, S. C. Lee, F. Licausi, P. Perata, L. A. C. J. Voesenek and J. T. van Dongen, *Trends Plant Sci.*, 2012, **17**, 129–138.
10 A. E. Little, C. J. Robinson, S. B. Peterson, K. F. Raffa and J. Handelsman, *Annu. Rev. Microbiol.*, 2008, **62**, 375–401.
11 R. Battino, T. R. Rettich and T. Tominaga, *The solubility of oxygen and ozone in liquids*, American Chemical Society and the American Institute of Physics for the National Bureau of Standards, 1983.
12 S. Fischkoff and J. Vanderkooi, *J. Gen. Physiol.*, 1975, **65**, 663–676.
13 S. M. Borisov and O. S. Wolfbeis, *Chem. Rev.*, 2008, **108**, 423.
14 C. McDonagh, C. S. Burke and B. D. MacCraith, *Chem. Rev.*, 2008, **108**, 400.
15 G. Orellana and D. Haigh, *Curr. Anal. Chem.*, 2008, **4**, 273–295.
16 M. Quaranta, S. M. Borisov and I. Klimant, *Bioanal. Rev.*, 2012, **4**, 115–157.
17 Y. Amao and I. Okura, *J. Porphyrins Phthalocyanines*, 2009, **13**, 1111–1122.
18 R. I. Dmitriev and D. B. Papkovsky, *Cell. Mol. Life Sci.*, 2012, **69**, 2025–2039.
19 X.-d. Wang, H.-x. Chen, Y. Zhao, X. Chen and X.-r. Wang, *TrAC, Trends Anal. Chem.*, 2010, **29**, 319–338.
20 X.-D. Wang and O. S. Wolfbeis, *Anal. Chem.*, 2012, **85**, 487–508.
21 Y. Feng, J. Cheng, L. Zhou, X. Zhou and H. Xiang, *Analyst*, 2012, **137**, 4885–4901.
22 L. W. Winkler, *Ber. Dtsch. Chem. Ges.*, 1888, **21**, 2843–2854.
23 R. O. Howard, D. W. Richardson, M. H. Smith and J. L. Patterson Jr, *Circ. Res.*, 1965, **16**, 187–196.
24 D. D. Van Slyke and J. M. Neill, *J. Biol. Chem.*, 1924, **61**, 523–573.
25 J. W. Swinnerton, V. J. Linnenbom and C. H. Cheek, *Anal. Chem.*, 1962, **34**, 483–485.
26 L. C. Clark, R. Wolf, D. Granger and Z. Taylor, *J. Appl. Physiol.*, 1953, **6**, 189–193.
27 H. J. Halpern, C. Yu, M. Peric, E. Barth, D. J. Grdina and B. A. Teicher, *Proc. Natl. Acad. Sci. U. S. A.*, 1994, **91**, 13047–13051.
28 M. D. Fox and M. E. Raichle, *Nat. Rev. Neurosci.*, 2007, **8**, 700–711.
29 G. Sette, J. Baron, B. Mazoyer, M. Levasseur, S. Pappata and C. Crouzel, *Brain*, 1989, **112**, 931–951.
30 T. Aoyagi, *J. Anesth.*, 2003, **17**, 259–266.
31 R. D. Frostig, E. E. Lieke, D. Y. Ts'o and A. Grinvald, *Proc. Natl. Acad. Sci. U. S. A.*, 1990, **87**, 6082–6086.
32 I. Bergman, *Nature*, 1968, **218**, 396.
33 J. M. Vanderkooi, G. Maniara, T. J. Green and D. F. Wilson, *J. Biol. Chem.*, 1987, **262**, 5476–5482.
34 M. B. Elowitz, M. G. Surette, P.-E. Wolf, J. Stock and S. Leibler, *Curr. Biol.*, 1997, **7**, 809–812.
35 R. Oshino, N. Oshino, M. Tamura, L. Kobilinsky and B. Chance, *Biochim. Biophys. Acta, Gen. Subj.*, 1972, **273**, 5–17.
36 S. Ashkenazi, S.-W. Huang, T. Horvath, Y.-E. L. Koo and R. Kopelman, *J. Biomed. Opt.*, 2008, **13**, 034023–034024.
37 E. G. Mik, J. Stap, M. Sinaasappel, J. F. Beek, J. A. Aten, T. G. van Leeuwen and C. Ince, *Nat. Methods*, 2006, **3**, 939–945.
38 M. A. Varia, D. P. Calkins-Adams, L. H. Rinker, A. S. Kennedy, D. B. Novotny, W. C. Fowler and J. A. Raleigh, *Gynecol. Oncol.*, 1998, **71**, 270–277.
39 J. Raleigh, A. Franko, C. Koch and J. Born, *Br. J. Cancer*, 1985, **51**, 229.
40 E. Takahashi, T. Takano, Y. Nomura, S. Okano, O. Nakajima and M. Sato, *Am. J. Physiol.: Cell Physiol.*, 2006, **291**, C781–C787.
41 H. Kautsky and A. Hirsch, *Z. Anorg. Allg. Chem.*, 1935, **222**, 126–134.
42 W. Vaughn and G. Weber, *Biochemistry*, 1970, **9**, 464–473.
43 I. Longmuir and J. A. Knopp, *J. Appl. Physiol.*, 1976, **41**, 598–602.
44 W. L. Rumsey, J. M. Vanderkooi and D. F. Wilson, *Science*, 1988, **241**, 1649–1651.
45 S. Das, A. M. Powe, G. A. Baker, B. Valle, B. El-Zahab, H. O. Sintim, M. Lowry, S. O. Fakayode, M. E. McCarroll, G. Patonay, M. Li, R. M. Strongin, M. L. Geng and I. M. Warner, *Anal. Chem.*, 2011, **84**, 597–625.
46 F. Giuntini, C. M. Alonso and R. W. Boyle, *Photochem. Photobiol. Sci.*, 2011, **10**, 759–791.
47 Y.-E. Koo Lee, R. Smith and R. Kopelman, *Annu. Rev. Anal. Chem.*, 2009, **2**, 57–76.
48 W. R. Algar, D. E. Prasuhn, M. H. Stewart, T. L. Jennings, J. B. Blanco-Canosa, P. E. Dawson and I. L. Medintz, *Bioconjugate Chem.*, 2011, **22**, 825–858.
49 B. A. Wilt, L. D. Burns, E. T. W. Ho, K. K. Ghosh, E. A. Mukamel and M. J. Schnitzer, *Annu. Rev. Neurosci.*, 2009, **32**, 435.
50 S. van de Linde, M. Heilemann and M. Sauer, *Annu. Rev. Phys. Chem.*, 2012, **63**, 519–540.
51 M. Y. Berezin and S. Achilefu, *Chem. Rev.*, 2010, **110**, 2641.
52 M. I. J. Stich, L. H. Fischer and O. S. Wolfbeis, *Chem. Soc. Rev.*, 2010, **39**, 3102–3114.
53 O. S. Wolfbeis, *Anal. Chem.*, 2006, **78**, 3859.
54 D. B. Papkovsky and T. C. O'Riordan, *J. Fluoresc.*, 2005, **15**, 569–584.
55 A. Krasnovsky, *Photochem. Photobiol.*, 1979, **29**, 29–36.
56 S. Mitra and T. H. Foster, *Biophys. J.*, 2000, **78**, 2597–2605.
57 A. Ruggi, F. W. B. van Leeuwen and A. H. Velders, *Coord. Chem. Rev.*, 2011, **255**, 2542–2554.

Published on 18 June 2013. Downloaded by University College Cork on 18/06/2013 10:57:28.

58 R. P. Brinas, T. Troxler, R. M. Hochstrasser and S. A. Vinogradov, *J. Am. Chem. Soc.*, 2005, **127**, 11851–11862.
59 O. S. Finikova, A. Y. Lebedev, A. Aprelev, T. Troxler, F. Gao, C. Garnacho, S. Muro, R. M. Hochstrasser and S. A. Vinogradov, *ChemPhysChem*, 2008, **9**, 1673–1679.
60 A. Y. Lebedev, T. Troxler and S. A. Vinogradov, *J. Porphyrins Phthalocyanines*, 2008, **12**, 1261–1269.
61 I. Dunphy, S. A. Vinogradov and D. F. Wilson, *Anal. Biochem.*, 2002, **310**, 191–198.
62 L.-W. Lo, C. J. Koch and D. F. Wilson, *Anal. Biochem.*, 1996, **236**, 153–160.
63 Y. Amao, *Microchim. Acta*, 2003, **143**, 1–12.
64 T. V. Esipova, A. Karagodov, J. Miller, D. F. Wilson, T. M. Busch and S. A. Vinogradov, *Anal. Chem.*, 2011, **83**, 8756–8765.
65 P. Chojnacki, G. Mistlberger and I. Klimant, *Angew. Chem.*, 2007, **119**, 9006–9009.
66 O. Stern and M. Volmer, *Phys. Z.*, 1919, **20**, 183–188.
67 E. R. Carraway, J. N. Demas, B. A. DeGraff and J. R. Bacon, *Anal. Chem.*, 1991, **63**, 337–342.
68 H. Xu, J. W. Aylott, R. Kopelman, T. J. Miller and M. A. Philbert, *Anal. Chem.*, 2001, **73**, 4124–4133.
69 N. W. Choi, S. S. Verbridge, R. M. Williams, J. Chen, J.-Y. Kim, R. Schmehl, C. E. Farnum, W. R. Zipfel, C. Fischbach and A. D. Stroock, *Biomaterials*, 2012, **33**, 2710–2722.
70 A. Fercher, A. Zhdanov and D. Papkovsky, *Phosphorescent Oxygen-Sensitive Probes*, Springer, Basel, 2012, pp. 71–101.
71 D. B. Papkovsky, *Methods Enzymol.*, 2004, **381**, 715–735.
72 A. Duerkop, M. Schaeferling and O. S. Wolfbeis, *Glucose Sensing*, 2006, vol. 11, pp. 351–375.
73 S. Sakadzic, E. Roussakis, M. A. Yaseen, E. T. Mandeville, V. J. Srinivasan, K. Arai, S. Ruvinskaya, A. Devor, E. H. Lo, S. A. Vinogradov and D. A. Boas, *Nat. Methods*, 2010, **7**, 755–759.
74 D. F. Wilson, O. S. Finikova, A. Y. Lebedev, S. Apreleva, A. Pastuszko, W. M. F. Lee and S. A. Vinogradov, *Oxygen Transport to Tissue XXXII*, Springer, US, 2011, vol. 701, pp. 53–59.
75 A. Devor, S. Sakadzic, V. J. Srinivasan, M. A. Yaseen, K. Nizar, P. A. Saisan, P. Tian, A. M. Dale, S. A. Vinogradov, M. A. Franceschini and D. A. Boas, *J. Cereb. Blood Flow Metab.*, 2012, **32**, 1259–1276.
76 Y. Liu, H. Guo and J. Zhao, *Chem. Commun.*, 2011, **47**, 11471–11473.
77 H. Xiang, L. Zhou, Y. Feng, J. Cheng, D. Wu and X. Zhou, *Inorg. Chem.*, 2012, **51**, 5208–5212.
78 W. Becker, A. Bergmann and C. Biskup, *Microsc. Res. Tech.*, 2007, **70**, 403–409.
79 O. S. Wolfbeis, *Anal. Chem.*, 2008, **80**, 4269–4283.
80 A. S. Golub and R. N. Pittman, *Am. J. Physiol.: Heart Circ. Physiol.*, 2008, **294**, H2905–H2916.
81 N. López-Ruiz, A. Martínez-Olmos, I. Vargas-Sansalvador, M. Fernández-Ramos, M. Carvajal, L. Capitán-Vallvey and A. Palma, *Sens. Actuators, B*, 2012, **171–172**, 938–945.
82 B. Ungerböck, V. Charwat, P. Ertl and T. Mayr, *Lab Chip*, 2013, **13**, 1593–1601.
83 Š. Zajko and I. Klimant, *Sens. Actuators, B*, 2013, **177**, 86–93.
84 J. Chapman, E. Weir and F. Regan, *Colloids Surf., B*, 2010, **78**, 208–216.
85 M.-S. Steiner, A. Duerkop and O. S. Wolfbeis, *Chem. Soc. Rev.*, 2011, **40**, 4805–4839.
86 J. Wang, *Chem. Rev.*, 2008, **108**, 814.
87 A. Pasic, H. Koehler, I. Klimant and L. Schaupp, *Sens. Actuators, B*, 2007, **122**, 60–68.
88 E. Ortega, S. de Marcos and J. Galbán, *Biosens. Bioelectron.*, 2012, **41**, 150–156.
89 J. Hynes, L. D. Marroquin, V. I. Ogurtsov, K. N. Christiansen, G. J. Stevens, D. B. Papkovsky and Y. Will, *Toxicol. Sci.*, 2006, **92**, 186–200.
90 R. M. Ballew and J. Demas, *Anal. Chem.*, 1989, **61**, 30–33.
91 T. C. O'Riordan, A. V. Zhdanov, G. V. Ponomarev and D. B. Papkovsky, *Anal. Chem.*, 2007, **79**, 9414–9419.
92 J. Hynes, E. Natoli Jr and Y. Will, *Curr. Protoc. Toxicol.*, 2009, ch. 2, Unit 2 16.
93 A. Zitova, J. Hynes, J. Kollar, S. M. Borisov, I. Klimant and D. B. Papkovsky, *Anal. Biochem.*, 2010, **397**, 144–151.
94 A. Zitova, F. C. O'Mahony, I. N. Kurochkin and D. B. Papkovsky, *Anal. Lett.*, 2010, **43**, 1746–1755.
95 F. S. Ligler and C. R. Taitt, *Optical biosensors: today and tomorrow*, Elsevier Science, 2011.
96 C. G. Perry, D. A. Kane, I. R. Lanza and P. D. Neufer, *Diabetes*, 2013, **62**, 1041–1053.
97 K. A. Foster, F. Galeffi, F. J. Gerich, D. A. Turner and M. Müller, *Prog. Neurobiol.*, 2006, **79**, 136–171.
98 Y. Will, J. Hynes, V. I. Ogurtsov and D. B. Papkovsky, *Nat. Protoc.*, 2007, **1**, 2563–2572.
99 D. F. Wilson, D. K. Harrison and S. A. Vinogradov, *J. Appl. Physiol.*, 2012, **113**, 1838–1845.
100 M. Porceddu, N. Buron, C. Roussel, G. Labbe, B. Fromenty and A. Borgne-Sanchez, *Toxicol. Sci.*, 2012, **129**, 332–345.
101 A. Heller, L. H. Fischer, O. S. Wolfbeis and A. Göpferich, *Exp. Cell Res.*, 2012, **318**, 1667–1672.
102 G. W. Rogers, M. D. Brand, S. Petrosyan, D. Ashok, A. A. Elorza, D. A. Ferrick and A. N. Murphy, *PLoS One*, 2011, **6**, e21746.
103 J. Hynes, S. Nadanaciva, R. Swiss, C. Carey, S. Kirwan and Y. Will, *Toxicol. In Vitro*, 2013, **27**, 560–569.
104 J. Hynes, T. C. O'Riordan, A. V. Zhdanov, G. Uray, Y. Will and D. B. Papkovsky, *Anal. Biochem.*, 2009, **390**, 21–28.
105 D. A. Ferrick, A. Neilson and C. Beeson, *Drug Discovery Today*, 2008, **13**, 268–274.
106 A. A. Gerencser, A. Neilson, S. W. Choi, U. Edman, N. Yadava, R. J. Oh, D. A. Ferrick, D. G. Nicholls and M. D. Brand, *Anal. Chem.*, 2009, **81**, 6868–6878.
107 J. Kim and R. C. Hayward, *Trends Biotechnol.*, 2012, **30**, 426–439.
108 P. A. Marichal-Gallardo and M. M. Álvarez, *Biotechnol. Prog.*, 2012, **28**, 899–916.
109 S. Nadanaciva and Y. Will, *Curr. Pharm. Des.*, 2011, **17**, 2100–2112.
110 C. E. Thomas and Y. Will, *Expert Opin. Drug Discovery*, 2012, **7**, 109–122.

 This journal is © The Royal Society of Chemistry 2013

Published on 18 June 2013. Downloaded by University College Cork on 18/06/2013 10:57:28.

111 S. Nadanaciva, P. Rana, G. Beeson, D. Chen, D. Ferrick, C. Beeson and Y. Will, *J. Bioenerg. Biomembr.*, 2012, **44**, 421–437.
112 A. V. Zhdanov, R. I. Dmitriev and D. B. Papkovsky, *Cell. Mol. Life Sci.*, 2011, **68**, 903–917.
113 G. Jasionek, A. Zhdanov, J. Davenport, L. Bláha and D. B. Papkovsky, *Environ. Sci. Technol.*, 2010, **44**, 2535–2541.
114 A. Zhdanov, C. Favre, L. O'Flaherty, J. Adam, R. O'Connor, P. Pollard and D. Papkovsky, *Integr. Biol.*, 2011, **3**, 1135–1142.
115 C. Favre, A. Zhdanov, M. Leahy, D. Papkovsky and R. O'Connor, *Oncogene*, 2010, **29**, 3964–3976.
116 L. O'Flaherty, J. Adam, L. C. Heather, A. V. Zhdanov, Y. L. Chung, M. X. Miranda, J. Croft, S. Olpin, K. Clarke, C. W. Pugh, J. Griffiths, D. Papkovsky, H. Ashrafian, P. J. Ratcliffe and P. J. Pollard, *Hum. Mol. Genet.*, 2010, **19**, 3844–3851.
117 A. V. Zhdanov, R. I. Dmitriev, A. V. Golubeva, S. A. Gavrilova and D. B. Papkovsky, *Biochim. Biophys. Acta, Gen. Subj.*, 2013, **1830**, 3553–3569.
118 K. A. O'Hagan, S. Cocchiglia, A. V. Zhdanov, M. M. Tambuwala, E. P. Cummins, M. Monfared, T. A. Agbor, J. F. Garvey, D. B. Papkovsky, C. T. Taylor and B. B. Allan, *Proc. Natl. Acad. Sci. U. S. A.*, 2009, **106**, 2188–2193.
119 H. J. Sung, W. Ma, P. Wang, J. Hynes, T. C. O'Riordan, C. A. Combs, J. P. McCoy Jr, F. Bunz, J. G. Kang and P. M. Hwang, *Nat. Commun.*, 2010, **1**, 5.
120 C. Frezza, L. Zheng, D. A. Tennant, D. B. Papkovsky, B. A. Hedley, G. Kalna, D. G. Watson and E. Gottlieb, *PLoS One*, 2011, **6**, e24411.
121 T. D. Papkovskaia, K.-Y. Chau, F. Inesta-Vaquera, D. B. Papkovsky, D. G. Healy, K. Nishio, J. Staddon, M. R. Duchen, J. Hardy, A. H. V. Schapira and J. M. Cooper, *Hum. Mol. Genet.*, 2012, **21**, 4201–4213.
122 J. T. Newington, T. Rappon, S. Albers, D. Y. Wong, R. J. Rylett and R. C. Cumming, *J. Biol. Chem.*, 2012, **287**, 37245–37258.
123 Q. Dai, A. A. Shah, R. V. Garde, B. A. Yonish, L. Zhang, N. A. Medvitz, S. E. Miller, E. L. Hansen, C. N. Dunn and T. M. Price, *Mol. Endocrinol.*, 2013, **27**, 741–753.
124 K. J. Morten, L. Badder and H. J. Knowles, *J. Pathol.*, 2012, **229**, 755–764.
125 P. Clerc and B. M. Polster, *PLoS One*, 2012, **7**, e34465.
126 P. Rana, B. Anson, S. Engle and Y. Will, *Toxicol. Sci.*, 2012, **130**, 117–131.
127 M. P. Horan, N. Pichaud and J. W. O. Ballard, *J. Gerontol., Ser. A*, 2012, **67**, 1022–1035.
128 F. Pampaloni, E. G. Reynaud and E. H. Stelzer, *Nat. Rev. Mol. Cell Biol.*, 2007, **8**, 839–845.
129 M. M. Mason, *J. Bacteriol.*, 1935, **29**, 103.
130 T. M. Hoehler and B. B. Jorgensen, *Nat. Rev. Microbiol.*, 2013, **11**, 83–94.
131 D. T. Stitt, M. S. Nagar, T. A. Haq and M. R. Timmins, *BioTechniques*, 2002, **32**, 684, 686, 688.
132 F. C. O'Mahony and D. B. Papkovsky, *Appl. Environ. Microbiol.*, 2006, **72**, 1279–1287.
133 R. Fernandes, C. Carey, J. Hynes and D. Papkovsky, *J. AOAC Int.*, 2013, **96**, 369–385.
134 J. Morton, N. Karoonuthaisiri, L. Stewart, M. Oplatowska, C. Elliott and I. Grant, *J. Appl. Microbiol.*, 2013, DOI: 10.1111/jam.12207.
135 T. Maniatis, E. F. Fritsch and J. Sambrook, *Molecular cloning: a laboratory manual*, Cold Spring Harbor Laboratory, Cold Spring Harbor, NY, 1982.
136 D. Y. Fung, *Compr. Rev. Food Sci. Food Saf.*, 2002, **1**, 3–22.
137 G. Jasionek, V. Ogurtsov and D. Papkovsky, *J. Appl. Microbiol.*, 2013, **114**, 423–432.
138 R. J. Winzler, *J. Cell. Comp. Physiol.*, 1941, **17**, 263–276.
139 D. M. Troppens, R. I. Dmitriev, D. B. Papkovsky, F. O'Gara and J. P. Morrissey, *FEMS Yeast Res.*, 2013, **13**, 322–334.
140 M. Hernando, M. Ejerhoon, A. Fernandez-Alba and Y. Chisti, *Water Res.*, 2003, **37**, 4091–4098.
141 A. Zitova, G. Jasionek and D. B. Papkovsky, *Waste Water Evaluation and Management*, 2011, vol. 10, p. 21129.
142 K. Schouest, A. Zitova, C. Spillane and D. B. Papkovsky, *Environ. Toxicol. Chem.*, 2009, **28**, 791–799.
143 D. laboratories, *Difco manual: dehydrated culture media and reagents for microbiology*, Difco Laboratories, 1985.
144 R. Eden and G. Ruth, *Microbiological Research and Development for the Food Industry*, 2012, vol. 269.
145 J. Kim, J.-S. Hahn, M. J. Franklin, P. S. Stewart and J. Yoon, *J. Antimicrob. Chemother.*, 2009, **63**, 129–135.
146 M. Skolimowski, M. W. Nielsen, F. Abeille, P. Skafte-Pedersen, D. Sabourin, A. Fercher, D. Papkovsky, S. Molin, R. Taboryski, C. Sternberg, M. Dufva, O. Geschke and J. Emneus, *Biomicrofluidics*, 2012, **6**, 034109–034111.
147 M. Skolimowski, M. W. Nielsen, J. Emnéus, S. Molin, R. Taboryski, C. Sternberg, M. Dufva and O. Geschke, *Lab Chip*, 2010, **10**, 2162–2169.
148 M. A. Acosta, M. Velasquez, K. Williams, J. M. Ross and J. B. Leach, *Biotechnol. Bioeng.*, 2012, **109**, 2663–2670.
149 A. Mills, *Chem. Soc. Rev.*, 2005, **34**, 1003–1011.
150 S. R. Nugen and A. Baeumner, *Anal. Bioanal. Chem.*, 2008, **391**, 451–454.
151 C. Pénicaud, S. Peyron, N. Gontard and V. Guillard, *Food Rev. Int.*, 2012, **28**, 113–145.
152 A. Mills, K. Lawrie, J. Bardin, A. Apedaile, G. A. Skinner and C. O'Rourke, *Analyst*, 2012, **137**, 106–112.
153 N. Borchert, A. Hempel, H. Walsh, J. P. Kerry and D. B. Papkovsky, *Food Control*, 2012, **28**, 87–93.
154 A. W. Hempel, R. N. Gillanders, D. B. Papkovsky and J. P. Kerry, *Int. J. Dairy Technol.*, 2012, **65**, 456–460.
155 A. Hempel, N. Borchert, H. Walsh, K. Roy Choudhury, J. Kerry and D. Papkovsky, *J. Food Prot.*, 2011, **74**, 776–782.
156 S. Engelhard, M. U. Kumke and H. G. Löhmannsröben, *Anal. Bioanal. Chem.*, 2006, **384**, 1107–1112.
157 A. Hempel, M. O'Sullivan, D. Papkovsky and J. Kerry, *LWT–Food Sci. Technol.*, 2012, **50**, 226–231.
158 F. O'Mahony, R. A. Green, C. Baylis, R. Fernandes and D. B. Papkovsky, *Food Control*, 2009, **20**, 129–135.

Published on 18 June 2013. Downloaded by University College Cork on 18/06/2013 10:57:28.

159 M. Kramer, N. Obermajer, B. B. Matijašić, I. Rogelj and V. Kmetec, *Appl. Microbiol. Biotechnol.*, 2009, **84**, 1137–1147.
160 A. Hempel, M. O'Sullivan, D. Papkovsky and J. Kerry, *LWT–Food Sci. Technol.*, 2013, **50**, 226–231.
161 B. H. Kim, I. S. Chang, G. C. Gil, H. S. Park and H. J. Kim, *Biotechnol. Lett.*, 2003, **25**, 541–545.
162 J. K. Bready and S. Friedman, *J. Insect Physiol.*, 1963, **9**, 337–347.
163 L. Cleveland, *Biol. Bull.*, 1925, **48**, 455–468.
164 W. J. Bruyninckx and H. S. Mason, *Nature*, 1978, **274**, 606–607.
165 H. J. Sung, W. Ma, M. F. Starost, C. U. Lago, P. K. Lim, M. N. Sack, J.-G. Kang, P.-y. Wang and P. M. Hwang, *PLoS One*, 2011, **6**, e19785.
166 J. R. Totter, *Proc. Natl. Acad. Sci. U. S. A.*, 1980, **77**, 1763–1767.
167 B. Halliwell, *Biochem. Soc. Trans.*, 2007, **35**, 1147–1150.
168 S. Weber, A. Koch, J. Kankeleit, J.-C. Schewe, U. Siekmann, F. Stüber, A. Hoeft and S. Schröder, *Apoptosis*, 2009, **14**, 97–107.
169 O. Toussaint, G. Weemaels, F. D. Chainiaux, K. S. Kochanek and M. Wlaschek, *J. Cell. Physiol.*, 2011, **226**, 315–321.
170 B. Halliwell, *FEBS Lett.*, 2003, **540**, 3–6.
171 A. V. Zhdanov, V. I. Ogurtsov, C. T. Taylor and D. B. Papkovsky, *Integr. Biol.*, 2010, **2**, 443–451.
172 G. Mehta, A. Y. Hsiao, M. Ingram, G. D. Luker and S. Takayama, *J. Controlled Release*, 2012, **164**, 192–204.
173 S. M. Grist, L. Chrostowski and K. C. Cheung, *Sensors*, 2010, **10**, 9286–9316.
174 R. I. Dmitriev, A. V. Zhdanov, G. Jasionek and D. B. Papkovsky, *Anal. Chem.*, 2012, **84**, 2930–2938.
175 J. Dragavon, M. Amiri, B. Marteyn, P. Sansonetti and S. Shorte, *Proc. SPIE*, 2011, **7910**, DOI: 10.1117/12.875430.
176 J. Dragavon, T. Molter, C. Young, T. Strovas, S. McQuaide, M. Holl, M. Zhang, B. Cookson, A. Jen, M. Lidstrom, D. Meldrum and L. Burgess, *J. R. Soc. Interface*, 2008, **5**, S151–S159.
177 Y. E. Koo, Y. Cao, R. Kopelman, S. M. Koo, M. Brasuel and M. A. Philbert, *Anal. Chem.*, 2004, **76**, 2498–2505.
178 D. Sud and M.-A. Mycek, *J. Biomed. Opt.*, 2009, **14**, 020506.
179 A. Fercher, G. Ponomarev, D. Yashunski and D. Papkovsky, *Anal. Bioanal. Chem.*, 2010, **396**, 1793–1803.
180 C. Dolan, R. D. Moriarty, E. Lestini, M. Devocelle, R. J. Forster and T. E. Keyes, *J. Inorg. Biochem.*, 2013, **119**, 65–74.
181 A. Fercher, S. M. Borisov, A. V. Zhdanov, I. Klimant and D. B. Papkovsky, *ACS Nano*, 2011, **5**, 5499–5508.
182 T. Murase, T. Yoshihara and S. Tobita, *Chem. Lett.*, 2012, 262–263.
183 Y.-E. Koo Lee, E. E. Ulbrich, G. Kim, H. Hah, C. Strollo, W. Fan, R. Gurjar, S. Koo and R. Kopelman, *Anal. Chem.*, 2010, **82**, 8446–8455.
184 R. I. Dmitriev, A. V. Zhdanov, G. V. Ponomarev, D. V. Yashunski and D. B. Papkovsky, *Anal. Biochem.*, 2010, **398**, 24–33.
185 A. V. Zhdanov, M. W. Ward, C. T. Taylor, E. A. Souslova, D. M. Chudakov, J. H. Prehn and D. B. Papkovsky, *Biochim. Biophys. Acta*, 2010, **1797**, 1627–1637.
186 A. V. Zhdanov, R. I. Dmitriev and D. B. Papkovsky, *Biosci. Rep.*, 2012, **32**, 587–595.
187 T. Hagen, C. T. Taylor, F. Lam and S. Moncada, *Science*, 2003, **302**, 1975–1978.
188 E. Takahashi, H. Endoh and K. Doi, *Am. J. Physiol.*, 1999, **276**, H718–H724.
189 E. Takahashi, *Am. J. Physiol.: Heart Circ. Physiol.*, 2008, **294**, H2507–H2515.
190 E. Takahashi and M. Sato, *Intracellular Diffusion of Oxygen and Hypoxic Sensing: Role of Mitochondrial Respiration*, ed. I. Homma, Y. Fukuchi and H. Onimaru, Springer, New York, 2010, vol. 669, pp. 213–217.
191 R. I. Dmitriev, H. Ropiak, G. Ponomarev, D. V. Yashunsky and D. B. Papkovsky, *Bioconjugate Chem.*, 2011, **22**, 2507–2518.
192 A. V. Kondrashina, R. I. Dmitriev, S. M. Borisov, I. Klimant, I. O'Brien, Y. M. Nolan, A. V. Zhdanov and D. B. Papkovsky, *Adv. Funct. Mater.*, 2012, **22**, 4931–4939.
193 R. I. Dmitriev, A. V. Zhdanov, Y. M. Nolan and D. B. Papkovsky, *Stem Cells*, 2013, in press.
194 M. C. Hogan, *J. Appl. Physiol.*, 1999, **86**, 720–724.
195 R. A. Howlett, C. A. Kindig and M. C. Hogan, *J. Appl. Physiol.*, 2007, **102**, 1456–1461.
196 R. T. Hepple, R. A. Howlett, C. A. Kindig, C. M. Stary and M. C. Hogan, *Am. J. Physiol.: Regul., Integr. Comp. Physiol.*, 2010, **298**, R983–R988.
197 S. Koga, R. C. I. Wüst, B. Walsh, C. A. Kindig, H. B. Rossiter and M. C. Hogan, *Am. J. Physiol.: Regul., Integr. Comp. Physiol.*, 2013, **304**, R59–R66.
198 A. S. Golub, M. A. Tevald and R. N. Pittman, *Am. J. Physiol.: Heart Circ. Physiol.*, 2011, **300**, H135–H143.
199 A. S. Golub and R. N. Pittman, *Am. J. Physiol.: Heart Circ. Physiol.*, 2012, **303**, H47–H56.
200 W. Hiesinger, S. A. Vinogradov, P. Atluri, J. R. Fitzpatrick, J. R. Frederick, R. D. Levit, R. C. McCormick, J. R. Muenzer, E. C. Yang, N. A. Marotta, J. W. MacArthur, D. F. Wilson and Y. J. Woo, *J. Appl. Physiol.*, 2011, **110**, 1460–1465.
201 R. I. Dmitriev, H. M. Ropiak, D. V. Yashunsky, G. V. Ponomarev, A. V. Zhdanov and D. B. Papkovsky, *FEBS J.*, 2010, **277**, 4651–4661.
202 C. Wotzlaw, A. Bernardini, U. Berchner-Pfannschmidt, D. Papkovsky, H. Acker and J. Fandrey, *Am. J. Physiol.: Cell Physiol.*, 2011, **301**, C266–C271.
203 E. Schmälzlin, B. Walz, I. Klimant, B. Schewe and H. G. Löhmannsröben, *Sens. Actuators, B*, 2006, **119**, 251–254.
204 B. Schewe, E. Schmälzlin and B. Walz, *J. Exp. Biol.*, 2008, **211**, 805–815.
205 M. A. Acosta, P. Ymele-Leki, Y. V. Kostov and J. B. Leach, *Biomaterials*, 2009, **30**, 3068–3074.
206 D. Lambrechts, M. Roeffaers, G. Kerckhofs, S. J. Roberts, J. Hofkens, T. Van de Putte, H. Van Oosterwyck and J. Schrooten, *Biomaterials*, 2013, **34**, 922–929.
207 L. Wang, M. A. Acosta, J. B. Leach and R. L. Carrier, *Lab Chip*, 2013, **13**, 1586–1592.
208 A. Dragu, C. D. Taeger, R. Buchholz, B. Sommerfeld, H. Hübner, T. Birkholz, J. A. Kleinmann, F. Münch,

 This journal is © The Royal Society of Chemistry 2013

Published on 18 June 2013. Downloaded by University College Cork on 18/06/2013 10:57:28.

R. E. Horch and K. Präbst, *Arch. Orthop. Trauma. Surg.*, 2012, **132**, 655–661.
209 B. P. Weegman, V. A. Kirchner, W. E. Scott Iii, E. S. Avgoustiniatos, T. M. Suszynski, J. Ferrer-Fabrega, M. D. Rizzari, L. S. Kidder, R. Kandaswamy, D. E. R. Sutherland and K. K. Papas, *Transplant. Proc.*, 2010, **42**, 2020–2023.
210 B. Olmeda, L. Villén, A. Cruz, G. Orellana and J. Perez-Gil, *Biochim. Biophys. Acta Biomembr.*, 2010, **1798**, 1281–1284.
211 A. Carreau, B. El Hafny-Rahbi, A. Matejuk, C. Grillon and C. Kieda, *J. Cell. Mol. Med.*, 2011, **15**, 1239–1253.
212 P. D. Wagner, *Eur. J. Appl. Physiol.*, 2012, **112**, 1–8.
213 F. Palm and L. Nordquist, *Am. J. Physiol.: Regul., Integr. Comp. Physiol.*, 2011, **301**, R1229–R1241.
214 S. Schreml, R. Szeimies, L. Prantl, S. Karrer, M. Landthaler and P. Babilas, *Br. J. Dermatol.*, 2010, **163**, 257–268.
215 L. De Filippis and D. Delia, *Cell. Mol. Life Sci.*, 2011, **68**, 2831–2844.
216 S. N. Jespersen and L. Ostergaard, *J. Cereb. Blood Flow Metab.*, 2012, **32**, 264–277.
217 R. Pittman, *Acta Physiol.*, 2011, **202**, 311–322.
218 M. C. Simon and B. Keith, *Nat. Rev. Mol. Cell Biol.*, 2008, **9**, 285–296.
219 A. A. Mamalis and D. L. Cochran, *Arch. Oral Biol.*, 2011, **56**, 1466–1475.
220 A. Devor, S. Sakadžić, P. A. Saisan, M. A. Yaseen, E. Roussakis, V. J. Srinivasan, S. A. Vinogradov, B. R. Rosen, R. B. Buxton, A. M. Dale and D. A. Boas, *J. Neurosci.*, 2011, **31**, 13676–13681.
221 S. V. Apreleva, D. F. Wilson and S. A. Vinogradov, *Opt. Lett.*, 2006, **31**, 1082–1084.
222 A. Y. Lebedev, A. V. Cheprakov, S. Sakadzic, D. A. Boas, D. F. Wilson and S. A. Vinogradov, *ACS Appl. Mater. Interfaces*, 2009, **1**, 1292–1304.
223 T. J. Huppert, M. S. Allen, H. Benav, P. B. Jones and D. A. Boas, *J. Cereb. Blood Flow Metab.*, 2007, **27**, 1262–1279.
224 J. Lecoq, A. Parpaleix, E. Roussakis, M. Ducros, Y. G. Houssen, S. A. Vinogradov and S. Charpak, *Nat. Med.*, 2011, **17**, 893–898.
225 A. Parpaleix, Y. G. Houssen and S. Charpak, *Nat. Med.*, 2013, **19**, 241–246.
226 L. I. Cárdenas-Navia, D. Mace, R. A. Richardson, D. F. Wilson, S. Shan and M. W. Dewhirst, *Cancer Res.*, 2008, **68**, 5812–5819.
227 Y. Kano, D. C. Poole, M. Sudo, T. Hirachi, S. Miura and O. Ezaki, *Am. J. Physiol.: Regul., Integr. Comp. Physiol.*, 2011, **301**, R1350–R1357.
228 R. D. Shonat and A. C. Kight, *Ann. Biomed. Eng.*, 2003, **31**, 1084–1096.
229 S. V. Apreleva, D. F. Wilson and S. A. Vinogradov, *Appl. Opt.*, 2006, **45**, 8547–8559.
230 A. S. Golub, M. C. Barker and R. N. Pittman, *Am. J. Physiol.: Heart Circ. Physiol.*, 2007, **293**, H1097–H1106.
231 A. G. Tsai, B. Friesenecker, M. C. Mazzoni, H. Kerger, D. G. Buerk, P. C. Johnson and M. Intaglietta, *Proc. Natl. Acad. Sci. U. S. A.*, 1998, **95**, 6590–6595.
232 A. S. Golub, B. K. Song and R. N. Pittman, *Am. J. Physiol.: Heart Circ. Physiol.*, 2011, **301**, H737–H745.
233 D. F. Wilson, S. A. Vinogradov, P. Grosul, N. Sund, M. N. Vacarezza and J. Bennett, *Oxygen Transport to Tissue XXVII*, Springer, US, 2006, vol. 578, pp. 119–124.
234 D. F. Wilson, S. A. Vinogradov, P. Grosul, M. N. Vaccarezza, A. Kuroki and J. Bennett, *Appl. Opt.*, 2005, **44**, 5239–5248.
235 A. Shakoor, N. P. Blair, M. Mori and M. Shahidi, *Invest. Ophthalmol. Visual Sci.*, 2006, **47**, 4962–4965.
236 M. Shahidi, J. Wanek, N. P. Blair and M. Mori, *Invest. Ophthalmol. Visual Sci.*, 2009, **50**, 820–825.
237 T. K. Stepinac, S. R. Chamot, E. Rungger-Brändle, P. Ferrez, J.-L. Munoz, H. van den Bergh, C. E. Riva, C. J. Pournaras and G. A. Wagnières, *Invest. Ophthalmol. Visual Sci.*, 2005, **46**, 956–966.
238 O. Ergeneman, G. Dogangil, J. J. Abbott, M. K. Nazeeruddin and B. J. Nelson, Engineering in Medicine and Biology Society, 2007. EMBS 2007. 29th Annual International Conference of the IEEE, 2007.
239 K. A. Krohn, J. M. Link and R. P. Mason, *J. Nucl. Med.*, 2008, **49**, 129S–148S.
240 H. Maeda, *Adv. Enzyme Regul.*, 2001, **41**, 189–207.
241 J. Napp, T. Behnke, L. Fischer, C. Würth, M. Wottawa, D. M. Katschinski, F. Alves, U. Resch-Genger and M. Schäferling, *Anal. Chem.*, 2011, **83**, 9039–9046.
242 A. D. Estrada, A. Ponticorvo, T. N. Ford and A. K. Dunn, *Opt. Lett.*, 2008, **33**, 1038–1040.
243 Q. Fang, S. Sakadzic, L. Ruvinskaya, A. Devor, A. M. Dale and D. A. Boas, *Opt. Express*, 2008, **16**, 17530–17541.
244 P. Babilas, G. Liebsch, V. Schacht, I. Klimant, O. S. Wolfbeis, R. Szeimies and C. Abels, *Microcirculation*, 2005, **12**, 477–487.
245 P. Babilas, P. Lamby, L. Prantl, S. Schreml, E. M. Jung, G. Liebsch, O. S. Wolfbeis, M. Landthaler, R. M. Szeimies and C. Abels, *Skin Res. Technol.*, 2008, **14**, 304–311.
246 S. Schreml, R. J. Meier, O. S. Wolfbeis, T. Maisch, R. M. Szeimies, M. Landthaler, J. Regensburger, F. Santarelli, I. Klimant and P. Babilas, *Exp. Dermatol.*, 2011, **20**, 550–554.
247 J. Warnat, G. Liebsch, E. M. Stoerr, A. Brawanski and C. Woertgen, *Acta Neurochir.*, 2009, 185–188.
248 M. Galler, S. Moritz, G. Liebsch, C. Woertgen, A. Brawanski and J. Warnat, *Acta Neurochir.*, 2010, **152**, 2175–2182.
249 J. M. Ingram, C. Zhang, J. Xu and S. J. Schiff, *J. Neurosci. Methods*, 2013, **214**, 45–51.
250 D. Wilson, S. Vinogradov, G. Schears, T. Esipova and A. Pastuszko, in *Oxygen Transport to Tissue XXXIII*, ed. M. Wolf, H. U. Bucher, M. Rudin, S. Van Huffel, U. Wolf, D. F. Bruley and D. K. Harrison, Springer, US, 2012, vol. 737, pp. 221–227.
251 V. Tsytsarev, E. Pumbo, S. Borisov, H. Arakawa, R. S. Erzurumlu and D. B. Papkovsky, *J. Neurosci. Methods*, 2013, **216**, 146–151.
252 S. Zhang, M. Hosaka, T. Yoshihara, K. Negishi, Y. Iida, S. Tobita and T. Takeuchi, *Cancer Res.*, 2010, **70**, 4490–4498.

Published on 18 June 2013. Downloaded by University College Cork on 18/06/2013 10:57:28.

253 T. Yoshihara, Y. Yamaguchi, M. Hosaka, T. Takeuchi and S. Tobita, *Angew. Chem., Int. Ed.*, 2012, **51**, 4148–4151.
254 H. Komatsu, K. Yoshihara, H. Yamada, Y. Kimura, A. Son, S.-i. Nishimoto and K. Tanabe, *Chem.–Eur. J.*, 2013, **19**, 1971–1977.
255 B. Krammer and K. Plaetzer, *Photochem. Photobiol. Sci.*, 2008, **7**, 283–289.
256 S. I. A. Bodmer, G. M. Balestra, F. A. Harms, T. Johannes, N. J. H. Raat, R. J. Stolker and E. G. Mik, *J. Biophotonics*, 2012, **5**, 140–151.
257 F. A. Harms, W. M. de Boon, G. M. Balestra, S. I. Bodmer, T. Johannes, R. J. Stolker and E. G. Mik, *J. Biophotonics*, 2011, **4**, 731–739.
258 F. A. Harms, W. J. Voorbeijtel, S. I. Bodmer, N. J. Raat and E. G. Mik, *Mitochondrion*, 2012, DOI: 10.1016/j.mito.2012.10.005.
259 E. G. Mik, C. Ince, O. Eerbeek, A. Heinen, J. Stap, B. Hooibrink, C. A. Schumacher, G. M. Balestra, T. Johannes, J. F. Beek, A. F. Nieuwenhuis, P. van Horssen, J. A. Spaan and C. J. Zuurbier, *J. Mol. Cell. Cardiol.*, 2009, **46**, 943–951.
260 E. G. Mik, T. Johannes, C. J. Zuurbier, A. Heinen, J. H. P. M. Houben-Weerts, G. M. Balestra, J. Stap, J. F. Beek and C. Ince, *Biophys. J.*, 2008, **95**, 3977–3990.
261 Q. Peng, K. Berg, J. Moan, M. Kongshaug and J. M. Nesland, *Photochem. Photobiol.*, 1997, **65**, 235–251.
262 F. Piffaretti, A. M. Novello, R. S. Kumar, E. Forte, C. Paulou, P. Nowak-Sliwinska, H. van den Bergh and G. Wagnières, *J. Biomed. Opt.*, 2012, **17**, 115007.
263 C. Ast, E. Schmälzlin, H.-G. Löhmannsröben and J. T. van Dongen, *Sensors*, 2012, **12**, 7015–7032.
264 S. N. Oliver, J. E. Lunn, E. Urbanczyk-Wochniak, A. Lytovchenko, J. T. Van Dongen, B. Faix, E. Schmälzlin, A. R. Fernie and P. Geigenberger, *Plant Physiol.*, 2008, **148**, 1640–1654.
265 F. Licausi, F. M. Giorgi, E. Schmälzlin, B. Usadel, P. Perata, J. T. van Dongen and P. Geigenberger, *Plant Cell Physiol.*, 2011, **52**, 1957–1972.
266 E. Schmälzlin, J. T. van Dongen, I. Klimant, B. Marmodée, M. Steup, J. Fisahn, P. Geigenberger and H.-G. Löhmannsröben, *Biophys. J.*, 2005, **89**, 1339–1345.
267 A. Zabalza, J. T. Van Dongen, A. Froehlich, S. N. Oliver, B. Faix, K. J. Gupta, E. Schmälzlin, M. Igal, L. Orcaray and M. Royuela, *Plant Physiol.*, 2009, **149**, 1087–1098.
268 H. Tschiersch, G. Liebsch, L. Borisjuk, A. Stangelmayer and H. Rolletschek, *New Phytol.*, 2012, **196**, 926–936.
269 H. Tschiersch, G. Liebsch, A. Stangelmayer, L. Borisjuk and H. Rolletschek, *Microsensors*, 2011, ch. 13.
270 A. D. Berry and S. A. Sargent, *Postharvest Biol. Technol.*, 2009, **52**, 240–242.
271 O. K. Atkin and D. Macherel, *Ann. Bot.*, 2009, **103**, 581–597.
272 N. Rudolph, H. G. Esser, A. Carminati, A. B. Moradi, A. Hilger, N. Kardjilov, S. Nagl and S. E. Oswald, *J. Soils Sediments*, 2012, **12**, 63–74.
273 M. Adler, M. Polinkovsky, E. Gutierrez and A. Groisman, *Lab Chip*, 2010, **10**, 388–391.
274 J. Chen, H. D. Kim and K. C. Kim, *Microfluid. Nanofluid.*, 2013, **14**, 541–550.
275 G. Mehta, K. Mehta, D. Sud, J. W. Song, T. Bersano-Begey, N. Futai, Y. S. Heo, M. A. Mycek, J. J. Linderman and S. Takayama, *Biomed. Microdevices*, 2007, **9**, 123–134.
276 D. A. Ouattara, J.-M. Prot, A. Bunescu, M.-E. Dumas, B. Elena-Herrmann, E. Leclerc and C. Brochot, *Mol. BioSyst.*, 2012, **8**, 1908–1920.
277 P. C. Thomas, S. R. Raghavan and S. P. Forry, *Anal. Chem.*, 2011, **83**, 8821–8824.
278 R. H. W. Lam, M. C. Kim and T. Thorsen, *Anal. Chem.*, 2009, **81**, 5918–5924.
279 Y.-A. Chen, A. D. King, H.-C. Shih, C.-C. Peng, C.-Y. Wu, W.-H. Liao and Y.-C. Tung, *Lab Chip*, 2011, **11**, 3626–3633.
280 K. Funamoto, I. K. Zervantonakis, Y. Liu, C. J. Ochs, C. Kim and R. D. Kamm, *Lab Chip*, 2012, **12**, 4855.
281 M. Cioffi, J. Küffer, S. Ströbel, G. Dubini, I. Martin and D. Wendt, *J. Biomech. Eng.*, 2008, **41**, 2918–2925.
282 S. C. Oppegard, K. H. Nam, J. R. Carr, S. C. Skaalure and D. T. Eddington, *PLoS One*, 2009, **4**, e6891.
283 A. V. Kondrashina, D. B. Papkovsky and R. I. Dmitriev, *Analyst*, 2013, DOI: 10.1039/C3AN00658A.
284 S. Suresh, V. Srivastava and I. Mishra, *J. Chem. Technol. Biotechnol.*, 2009, **84**, 1091–1103.
285 A. S. Kocincová, S. Nagl, S. Arain, C. Krause, S. M. Borisov, M. Arnold and O. S. Wolfbeis, *Biotechnol. Bioeng.*, 2008, **100**, 430–438.
286 T. Klein, K. Schneider and E. Heinzle, *Biotechnol. Bioeng.*, 2013, **110**, 535–542.
287 F. Chen, Q. Xia and L. K. Ju, *Biotechnol. Bioeng.*, 2006, **93**, 1069–1078.
288 H. E. Abaci, R. Devendra, Q. Smith, S. Gerecht and G. Drazer, *Biomed. Microdevices*, 2012, **14**, 145–152.
289 R. Hortsch and D. Weuster-Botz, *Appl. Microbiol. Biotechnol.*, 2011, **90**, 69–76.
290 Y. Tian, B. R. Shumway, W. Gao, C. Youngbull, M. R. Holl, R. H. Johnson and D. R. Meldrum, *Sens. Actuators, B*, 2010, **150**, 579–587.
291 P. J. Cywinski, A. J. Moro, S. E. Stanca, C. Biskup and G. J. Mohr, *Sens. Actuators, B*, 2009, **135**, 472–477.
292 A. Zhdanov, J. Hynes, R. Dmitriev and D. Papkovsky, *Phosphorescent Oxygen-Sensitive Probes*, Springer, Basel, 2012, pp. 29–69.
293 A. Zitova, M. Cross, R. Hernan, J. Davenport and D. B. Papkovsky, *Chem. Ecol.*, 2009, **25**, 217–227.
294 A. Zitova, F. C. O'Mahony, M. Cross, J. Davenport and D. B. Papkovsky, *Environ. Toxicol.*, 2009, **24**, 116–127.
295 D. McKenzie, I. Lund and P. B. Pedersen, *Mar. Biol.*, 2008, **154**, 1041–1051.
296 J. Fabricius-Dyg, G. Mistlberger, M. Staal, S. M. Borisov, I. Klimant and M. Kühl, *Mar. Biol.*, 2012, **159**, 1621–1631.
297 H. Lu, Y. Jin, Y. Tian, W. Zhang, M. R. Holl and D. R. Meldrum, *J. Mater. Chem.*, 2011, **21**, 19293–19301.
298 G. U. Balcke, S. Wegener, B. Kiesel, D. Benndorf, M. Schlömann and C. Vogt, *Biodegradation*, 2008, **19**, 507–518.

 This journal is © The Royal Society of Chemistry 2013

Published on 18 June 2013. Downloaded by University College Cork on 18/06/2013 10:57:28.

299 T. Kragh, M. Søndergaard and L. Tranvik, *FEMS Microbiol. Ecol.*, 2008, **64**, 230–239.
300 K. E. Busch, P. Laurent, Z. Soltesz, R. J. Murphy, O. Faivre, B. Hedwig, M. Thomas, H. L. Smith and M. de Bono, *Nat. Neurosci.*, 2012, **15**, 581–591.
301 C. Scott, T. Lyons, A. Bekker, Y. Shen, S. Poulton, X. Chu and A. Anbar, *Nature*, 2008, **452**, 456–459.
302 M. Paumann, G. Regelsberger, C. Obinger and G. A. Peschek, *Biochim. Biophys. Acta, Bioenerg.*, 2005, **1707**, 231–253.
303 E. A. Bagshaw, J. L. Wadham, M. Mowlem, M. Tranter, J. Eveness, A. G. Fountain and J. Telling, *Environ. Sci. Technol.*, 2010, **45**, 700–705.
304 M. Kühl, L. Behrendt, E. C. L. Trampe, K. Qvortrup, U. Schreiber, S. M. Borisov, I. Klimant and A. W. D. Larkum, *Front. Microbiol.*, 2012, **3**, 402.
305 C. Baleizão, S. Nagl, M. Schäferling, M. r. N. Berberan-Santos and O. S. Wolfbeis, *Anal. Chem.*, 2008, **80**, 6449–6457.
306 S. Kochmann, C. Baleizão, M. N. Berberan-Santos and O. S. Wolfbeis, *Anal. Chem.*, 2013, **85**, 1300–1304.
307 T. S. Moore, K. M. Mullaugh, R. R. Holyoke, A. S. Madison, M. Yücel and G. W. Luther III, *Annu. Rev. Mar. Sci.*, 2009, **1**, 91–115.
308 L. Codispoti, J. A. Brandes, J. Christensen, A. Devol, S. Naqvi, H. W. Paerl and T. Yoshinari, *Sci. Mar.*, 2001, **65**, 85–105.
309 A. D. Sherman and K. Smith Jr., *Deep Sea Res., Part II*, 2009, **56**, 1754–1762.
310 A. Whitmire, R. Letelier, V. Villagrán and O. Ulloa, *Opt. Express*, 2009, **17**, 21992–22004.
311 H. Røy, J. Kallmeyer, R. R. Adhikari, R. Pockalny, B. B. Jørgensen and S. D'Hondt, *Science*, 2012, **336**, 922–925.
312 A. Stockdale, W. Davison and H. Zhang, *Earth-Sci. Rev.*, 2009, **92**, 81–97.
313 C. M. Haberer, M. Rolle, S. Liu, O. A. Cirpka and P. Grathwohl, *J. Contam. Hydrol.*, 2011, **122**, 26–39.
314 B. Finlay, *J. Gen. Microbiol.*, 1981, **123**, 173–178.
315 D. Hydes, M. Hartman, J. Kaiser and J. Campbell, *Estuarine, Coastal Shelf Sci.*, 2009, **83**, 485–490.
316 L. Chipman, M. Huettel, P. Berg, V. Meyer, I. Klimant, R. Glud and F. Wenzhoefer, *Limnol. Oceanogr.: Methods*, 2012, **10**, 304–316.
317 H. Uchida, T. Kawano, I. Kaneko and M. Fukasawa, *J. Atmos. Oceanic Technol.*, 2008, **25**, 2271–2281.
318 C. R. Schroeder, G. Neurauter and I. Klimant, *Microchim. Acta*, 2007, **158**, 205–218.
319 M. Warkentin, H. M. Freese, U. Karsten and R. Schumann, *Appl. Environ. Microbiol.*, 2007, **73**, 6722–6729.
320 V. I. Ogurtsov, J. Hynes, Y. Will and D. B. Papkovsky, *Sens. Actuators, B*, 2008, **129**, 581–590.
321 T. V. Esipova, X. Ye, J. E. Collins, S. Sakadžić, E. T. Mandeville, C. B. Murray and S. A. Vinogradov, *Proc. Natl. Acad. Sci. U. S. A.*, 2012, **109**, 20826–20831.
322 A. S. Golub, M. C. Barker and R. N. Pittman, *Am. J. Physiol.: Heart Circ. Physiol.*, 2007, **293**, H1097–H1106.
323 S. Geis, P. Babilas, S. Schreml, P. Angele, M. Nerlich, E. Jung and L. Prantl, *Clin. Hemorheol. Microcirc.*, 2008, **40**, 249–258.
324 J. M. Bolivar, T. Consolati, T. Mayr and B. Nidetzky, *Trends Biotechnol.*, 2013, **31**, 194–203.
325 J. S. Miller, K. R. Stevens, M. T. Yang, B. M. Baker, D.-H. T. Nguyen, D. M. Cohen, E. Toro, A. A. Chen, P. A. Galie and X. Yu, *Nat. Mater.*, 2012, **11**, 768–774.
326 F. Baldini, M. Bacci, F. Cosi and A. Del Bianco, *Sens. Actuators, B*, 1992, **7**, 752–757.
327 Z. Zhujun and W. R. Seitz, *Anal. Chem.*, 1986, **58**, 220–222.
328 R. Wolthuis, D. McCrae, E. Saaski, J. Hartl and G. Mitchell, *IEEE Trans. Biomed. Eng.*, 1992, **39**, 531–537.
329 M. L. Skiles, R. Fancy, P. Topiwala, S. Sahai and J. O. Blanchette, *J. Biomed. Mater. Res., Part B*, 2011, **97**, 148–155.
330 L. Cui, Y. Zhong, W. Zhu, Y. Xu, Q. Du, X. Wang, X. Qian and Y. Xiao, *Org. Lett.*, 2011, **13**, 928–931.
331 K. Kiyose, K. Hanaoka, D. Oushiki, T. Nakamura, M. Kajimura, M. Suematsu, H. Nishimatsu, T. Yamane, T. Terai and Y. Hirata, *J. Am. Chem. Soc.*, 2010, **132**, 15846–15848.
332 S. Takahashi, W. Piao, Y. Matsumura, T. Komatsu, T. Ueno, T. Terai, T. Kamachi, M. Kohno, T. Nagano and K. Hanaoka, *J. Am. Chem. Soc.*, 2012, **134**, 19588–19591.
333 J. Potzkei, M. Kunze, T. Drepper, T. Gensch, K.-E. Jaeger and J. Buechs, *BMC Biol.*, 2012, **10**, 28.
334 T. C. O'Riordan, A. E. Soini, J. T. Soini and D. B. Papkovsky, *Anal. Chem.*, 2002, **74**, 5845–5850.

View publication stats